FAKULTA MECHATRONIKY,
INFORMATIKY A MEZIOBOROVÝCH
STUDIÍ TUL

Bakalářská práce

Synthesis of selected bridged organosilane precursors suitable for the development of new hybrid nanofibres

Studijní program: B0719A130001 – Nanotechnologie
Autor práce: **Ondřej Haluza**
Vedoucí práce: Assoc. Prof., MSc. Veronika Máková, PhD
Konzultant: Christopher James Hobbs, PhD

Liberec 2023

FAKULTA MECHATRONIKY,
INFORMATIKY A MEZIOBOROVÝCH
STUDIÍ TUL

Zadání bakalářské práce

Synthesis of selected bridged organosilane precursors suitable for the development of new hybrid nanofibres

Jméno a příjmení:	**Ondřej Haluza**
Osobní číslo:	M20000143
Studijní program:	B0719A130001 Nanotechnologie
Zadávající katedra:	Katedra chemie
Akademický rok:	2022/2023

Zásady pro vypracování:

1. Synthesis of selected types of bridged organo-bis-silylated precursors.
2. Synthesis of their methylated bridged analogues.
3. Characterisation of prepared precursors via NMR, TGA, FTIR and mass spectrometry.
4. Formation of (nano)fibres from the synthesised precursors.

Rozsah grafických prací:	dle potřeby dokumentace
Rozsah pracovní zprávy:	30-40 stran
Forma zpracování práce:	tištěná/elektronická
Jazyk práce:	Angličtina

Seznam odborné literatury:

[1] V. Máková, B. Holubová, I. Krabicová, J. Kulhánková, M. Řezanka, Hybrid organosilane fibrous materials and their contribution to modern science, *Polymer*. **228** (2021) 123862. https://doi.org/10.1016/j.polymer.2021.123862.

[2] F. Rajabi, A.Z. Ebrahimi, A. Rabiee, A. Pineda, R. Luque, Synthesis and Characterization of Novel Pyridine Periodic Mesoporous Organosilicas and Its Catalytic Activity in the Knoevenagel Condensation Reaction. *Materials* (Basel). **13** (2020). https://doi.org/10.3390/ma13051097.

Vedoucí práce:	doc. Mgr. Veronika Máková, Ph.D. Katedra chemie
Datum zadání práce:	10. října 2022
Předpokládaný termín odevzdání:	22. května 2023

L.S.

prof. Ing. Zdeněk Plíva, Ph.D.
děkan

prof. Ing. Josef Šedlbauer, Ph.D.
vedoucí katedry

V Liberci dne 20. října 2022

Prohlášení

Prohlašuji, že svou bakalářskou práci jsem vypracoval samostatně jako původní dílo s použitím uvedené literatury a na základě konzultací s vedoucím mé bakalářské práce a konzultantem.

Jsem si vědom toho, že na mou bakalářskou práci se plně vztahuje zákon č. 121/2000 Sb., o právu autorském, zejména § 60 – školní dílo.

Beru na vědomí, že Technická univerzita v Liberci nezasahuje do mých autorských práv užitím mé bakalářské práce pro vnitřní potřebu Technické univerzity v Liberci.

Užiji-li bakalářskou práci nebo poskytnu-li licenci k jejímu využití, jsem si vědom povinnosti informovat o této skutečnosti Technickou univerzitu v Liberci; v tomto případě má Technická univerzita v Liberci právo ode mne požadovat úhradu nákladů, které vynaložila na vytvoření díla, až do jejich skutečné výše.

Současně čestně prohlašuji, že text elektronické podoby práce vložený do IS STAG se shoduje s textem tištěné podoby práce.

Beru na vědomí, že má bakalářská práce bude zveřejněna Technickou univerzitou v Liberci v souladu s § 47b zákona č. 111/1998 Sb., o vysokých školách a o změně a doplnění dalších zákonů (zákon o vysokých školách), ve znění pozdějších předpisů.

Jsem si vědom následků, které podle zákona o vysokých školách mohou vyplývat z porušení tohoto prohlášení.

22. 5. 2023 Ondřej Haluza

Syntéza vybraných přemostěných organosilanových prekurzorů vhodných pro vývoj nových hybridních nanovláken

Abstrakt

Cílem práce byla příprava přemostěných organosilanů, tzv. organo-bis-silylovaných prekurzorů s benzenovým, pyridinovým a oxalylovým organickým linkerem. Byly syntetizovány prekurzory vycházející z příslušných aminosilanů majících 1-2 methylové funkční skupiny namísto ethoxylových funkčních skupin. Byly použity syntetické postupy, jejichž produkty byly následně charakterizovány pomocí řady analytických technik, včetně NMR, hmotnostní spektrometrie, IČ a TGA. Nasyntetizované prekurzory byly převedeny do podoby (nano)vláken pomocí metod sol-gel a elektrostatického zvlákňování a následně charakterizovány pomocí metod NMR, SEM a IČ.
Klíčová slova: organosilany, organo-bis-silylované prekurzory, syntéza, sol-gel, elektrospinning, (nano)vlákna

Synthesis of selected bridged organosilane precursors suitable for the development of new hybrid nanofibres

Abstract

The aim of the work was to prepare bridged organosilanes, so-called organo-bis-silylated precursors with benzene, pyridine and oxalyl organic linkers. Precursors were synthesised from the respective aminosilanes having 1-2 methyl functional groups instead of ethoxy functional groups. Synthetic procedures were used and the products were subsequently characterised using analytical techniques, including NMR, mass spectrometry, IR and TGA. The synthesised precursors were transformed into the (nano)fibres with the help of methods of sol-gel and electrospinning. Subsequently, the prepared samples were successfully characterised through NMR, SEM and IR techniques.
Keywords: organosilanes, organo-bis-silylated precursors, synthesis, sol-gel, electrospinning, (nano)fibres

Acknowledgment

This way I would like to thank everyone who helped me either directly or indirectly. This thesis wouldn't be even possile without numerous people.

I would like to express my deepest appreciation and gratitude to my supervisor Assoc. Prof., MSc. Veronika Máková, PhD for her valuable guidance, encouragement, and support throughout my thesis. Her knowledge and enthusiasm had an invaluable asset on me.

I am also extremely grateful to Christopher James Hobbs, PhD, who has been with me every step of the way in the laboratory, providing me with valuable advices, feedbacks, and constant assistance. His dedications and especiall patience have been critical to the success of all the work.

Furthermore, I would like to acknowledge MSc. Johana Kulhánková for her help in getting started in the laboratory and her assistance in laboratory. Her support and help was essencial for this thesis as well.

I would also like to thank the laboratory staff for helping me through many characterisation methods. Their expertise and assistance were invaluable in helping me achieve my research objectives. I would like to thank PhD students for those advices, they helped me to achieve better results.

Finally, I would like to acknowledge the support and encouragement of my family and friends. Their love, understanding and patience have been my constant motivation throughout my academic journey. Without you all I won't be in the position I am now.

Contents

List of figures

List of tables

List of abbreviations

APTES	3-Aminopropyltriethoxysilane
APMDES	3-Aminopropylmethyldiethoxysilane
APDMES	3-Aminopropyldimethylethoxysilane
BiTSAP	*N,N'*-bis(3-(triethoxysilyl)propyl)pyridine-2,6-dicarboxyamide
BiTSAB-a	*N,N'*-bis(3-(triethoxysilyl)propyl)benzene-1,4-dicarboxyamide
BiTSAB-b	*N,N'*-bis(3-(diethoxy(methyl)silyl)propyl)benzene-1,4-dicarboxyamide
BiTSAB-c	*N,N'*-bis(3-(ethoxydimethylsilyl)propyl)benzene-1,4-dicarboxyamide
BTPO	*N,N'*-bis(3-(triethoxysilyl)propyl)ethanediamide
$(COCl)_2$	Oxalyl chloride
DCM	Dichloromethane
dH_2O	Distilled water
demi H_2O	Demineralized water
FTIR	Fourier transformation infrared spectroscopy
MS	Mass spectrometry
NMR	Nuclear magnetic resonance spectroscopy
PDC	2,6-Pyridinedicarbonyl dichloride
Rotovap	Rotary evaporator
SEM	Scanning electron microscopy
TEA	Triethylamine
TGA	Thermogravimetric analysis
TPC	Terephthaloyl chloride
RT	Room temperature

1 Introduction

Hybrid materials consisting of both organic and inorganic components have gained increasing attention in recent years due to their unique combination of properties. Among them, organosilane-based hybrid materials have been on particular interest as they show the promising prospects due to their potential applications in a wide range of fields of material science and everyday life. The sol-gel process belongs to one of the most common methods for preparing hybrid materials. Through the sol-gel polycondensation process they grow into a macromolecule siloxane polymer. Bridged organosilanes belong to the one of the most interesting hybrid materials. They may contain various types of organic linkers covalently bonded to silicon. Thus they have the ability to offer a variety of properties to the resulting hybrid organosilane material. The resulting material is characterised by the preservation of the major features of each part. Whilst the inorganic part contributes significantly to the mechanical properties and chemical stability of the hybrid material, the organic part provides properties such as biocompatibility, functionalization and/or conductivity (Kickelbick, 2007).

This thesis deals with the synthesis of new hybrid organosilane precursors and the formation of (nano)fibres. This research utilises various combinations of different organic linkers with various organosilanes. However, due to the large number of possible combinations of precursors, it was necessary to focus primarily on one organic linker with the various organosilane combinations for full characterisation and (nano)fibre formation.

2 Theoretical part

2.1 Hybrid materials

Since the beginning of industrial rise there were new challenges about combining properties of organic and inorganic compounds. These composite materials were made in order to improve their single part properties, with applications in fields such as the paint industry. In recent years, the focus has shifted towards the development of nanocomposites networks and gels, due to their versatility and potential use in a wide range of applications (Judeinstein and Sanchez, 1996).

Within the scientific community occurs another term that hybrid materials are connected to, known as hybrid nanocomposites. We need to well-define a border between hybrid nanocomposites and hybrid materials. Here is a gradual transition between inorganic-organic nanocomposites and inorganic-organic hybrid material that common knowledge states. Commonly the therm nanocomposites is used when discrete inorganic units, showed in the figure (2.1) below, are in specified size ranging from 1 to 100 nm, while these are incorporated usually in polymer organic units. In contrast, hybrid materials are commonly characterised using either inorganic or organic units produced *in situ* from molecular precursors, applying for example by the sol-gel reaction (Kickelbick, 2007) (Makova, Holubova, Krabicova, et al., 2021).

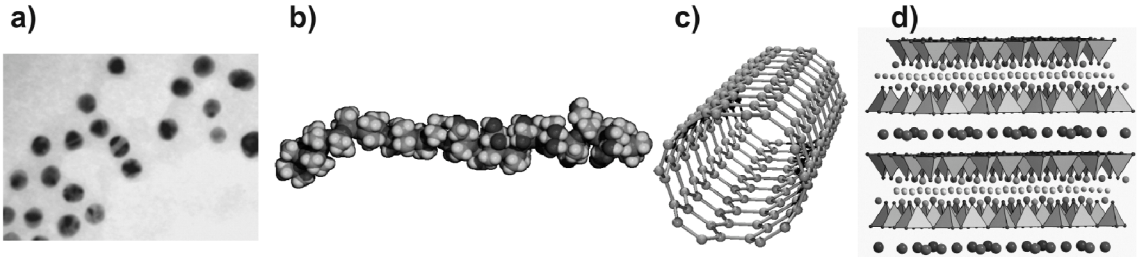

Figure 2.1: Inorganic building blocks used for organic-inorganic nanocomposite: a) nanoparticles, b) macromolecules, c) nanotubes, d) layered materials (Kickelbick, 2007).

Simply, hybrid material consists of two parts - organic and inorganic, which are blended on the nanometer scale. Commonly, one of these components is inorganic and the other is organic (Makova, Holubova, Krabicova, et al., 2021). The organic part can consist of molecular, oligomeric and macromolecular constituents, primarily

composed of hydrogen, carbon connected to a oxygen, nitrogen and halogens, while the inorganic part contains of an extensive range of metallic elements, typically in the form of oxides (D. Loy, 2007). Hybrid materials can be divided in two classes: Class I where organic and inorganic parts are connected with weak bonds (such as van der Waals forces, hydrogen bonds or electrostatic forces) and Class II where these parts are connected via strong interaction bonds (such as covalent bonds or iono-covalent bonds) (Makova, Holubova, Krabicova, et al., 2021)(Kickelbick, 2007).

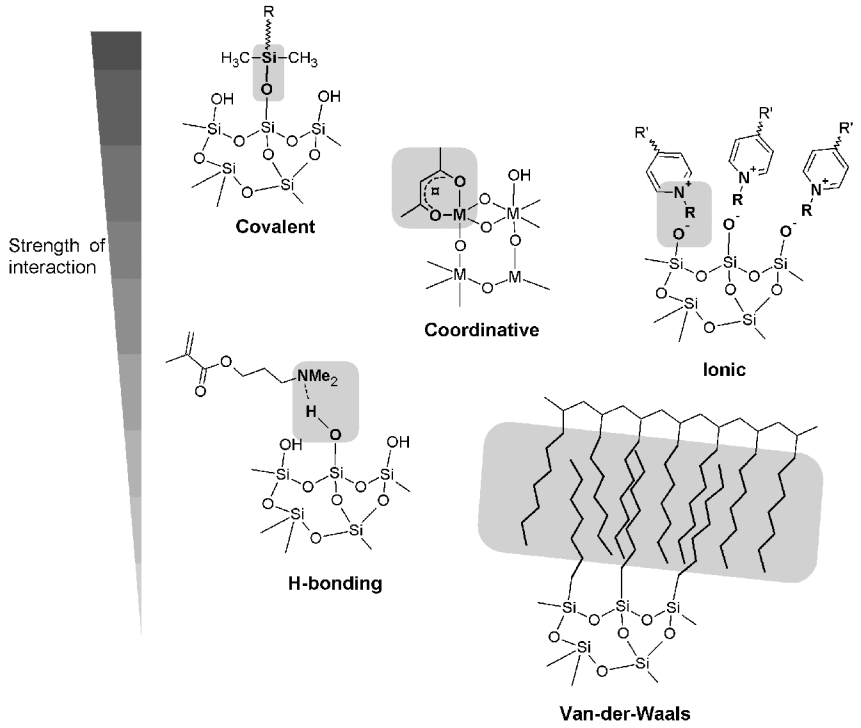

Figure 2.2: Examples of interactions that may occur in hybrid materials (Kickelbick, 2007).

2.1.1 Preparation of hybrid materials

There are numerous strategies leading for the preparation of hybrid materials and each method depends on the specific type of hybrid material and its intended application. However, there are two common approaches how to obtain the hybrid materials, including building block and *in situ* approach.

Building block approach

Using the building block approach, these building blocks can maintain the molecular integrity during the material formation. This means that the source unit is present in the final hybrid material, and that the characteristic properties of these building blocks can survive in the matrix. Modified inorganic clusters

or nanoparticles represent a class of well-defined building blocks, see figure (2.3). These clusters contain at least one reactive functional group reacting with the organic matrix, for example through copolymerisation. The number of interaction groups determines the ability to modify the organic matrix partially (only one functional group) or fully crosslinked materials (more than one functional group). If there are two functional groups connected to an inorganic cluster, there will be more a chain-like structure formation. However, three functional groups will tend to shape a highly cross-linked structure (Kickelbick, 2007).

Using this method for obtaining hybrid materials is very adaptable since we can adjust the building block units before the start of the reaction and thus integrate a desired property into the final hybrid material (Kickelbick, 2007).

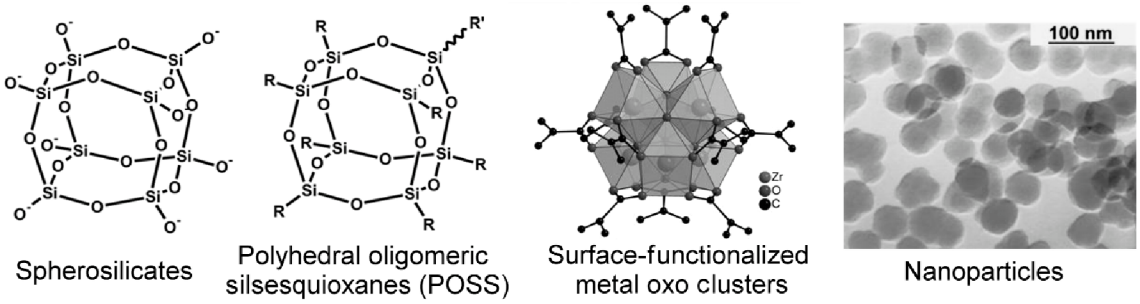

Figure 2.3: Examples of building blocks which can be used for hybrid materials formation (Kickelbick, 2007).

In situ approach

In comparison to building block approach, the *in situ* method involves the chemical transformation of the precursors. This approach is commonly used in the formation of organic polymers and inorganic components through the sol-gel process. During this process, the precursors tend to transform into multidimensional structures. Moreover, they often lose their previous properties and obtain new (unique) properties different from the original precursors. The internal structure of the final material is determined by the composition of the precursors and the reaction conditions. Control of these reaction parameters is essential in achieving the desired properties of hybrid materials. This means that even slight changes in reaction parameters (pH adjustment, the ratio of water to precursor, steric hindrance of the precursors) can lead to significant differences in the resulting materials.

The sol-gel process is a type of *in situ* approach suitable for synthesising hybrid materials fulfilling a few demands (mild temperatures, easy to adjust the reaction parameters). Due to the above-mentioned reasons, we have decided to use the sol-gel process, which is described in section 2.2.3.

Sol-gel

The sol-gel process is a widely used technique for generating dispersed inorganic substances in solvents. The chemistry of this process is based on inorganic polymerisation reactions (Judeinstein and Sanchez, 1996). This process involves the conversion of a precursor solution into a gel by a series of chemical reactions, where small molecules form due to polycondensation reaction polymeric structures by the loss of substituents (Kickelbick, 2007). The sol-gel process using metal alkoxides is a popular method for the synthesis of organic-inorganic hybrid materials. There are many metals that can be used for metal-alkoxides entering the sol-gel reaction such as silica, titania, alumina, vanadia, zirconia and germania, however silica stands out as the most convenient choice for many reasons (stable Si-C bonds, a well-documented sol-gel methodology ease of characterisation and commercially available starting materials) (Ogoshi and Chujo, 2005).

Sol-gel process is suitable for preparation of a wide variety of hybrid materials, because of its mild conditions. For example the organic components can't handle higher temperatures, generally over 250 °C, however sol-gel process overcomes this limitation by providing "soft" conditions. Sol-gel process offers numerous advantages such as easy control over the composition and structure of the resulting material, as well as the ability to incorporate a wide range of organic and inorganic components. The sol-gel process can be led to either a hydrolytic or non-hydrolytic way. This thesis has focused only on the hydrolytic approach (Makova, Holubova, Krabicova, et al., 2021)(Judeinstein and Sanchez, 1996)(Kickelbick, 2007).

The first step of the hydrolytic sol-gel process is the hydrolysis of metal-alkoxide, followed by a (poly)condensation reaction, see Figure (2.4).

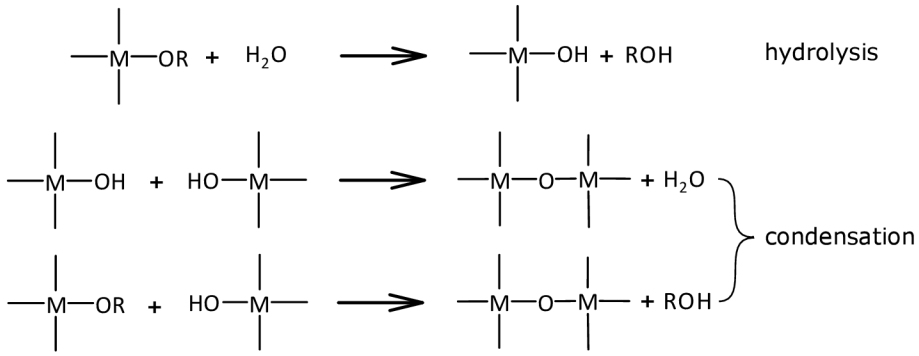

Figure 2.4: General scheme for sol-gel reaction mechanism, where M can be Si, Al, Ti, Zr, Ge etc.

These reactions result in the formation of metal-oxo oligomers and polymers that are in the end terminated with residual amount of hydroxo and/or alkyl groups (Judeinstein and Sanchez, 1996). There can also occur a polycondensation. The reaction mechanism can look as follow:

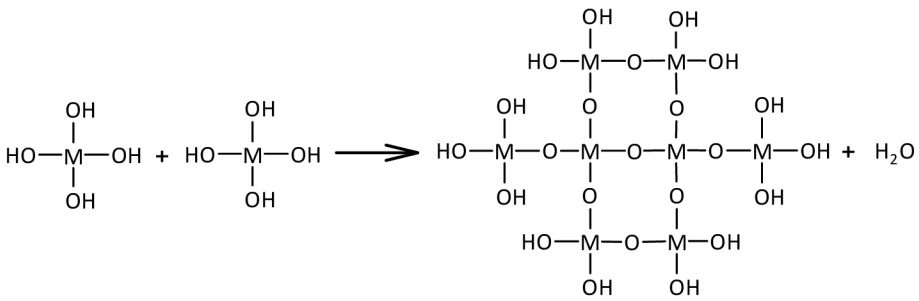

Figure 2.5: General scheme for polycondensation in various types of hybrid materials.

2.1.2 Properties of hybrid materials

The diverse spectrum of the properties of hybrid materials is influenced by the various types of synthetic approaches leading to their production (Judeinstein and Sanchez, 1996). Moreover, the nature of the interface, the interaction forces, the energy and the linkability between these components play the primary role in determining the properties of the resulting material (Makova, Holubova, Krabicova, et al., 2021).

The typically distinct properties of organic and inorganic compounds are in hybrid materials merged into a singular material. This field of study is remarkably innovative due to various combination of single properties of both parts allowing to formation of well-known and yet unknown characteristics (Kickelbick, 2007). In most cases there are major features of every phase that stay conserved within the hybrid materials with only minor adjustments expected to each phase's properties (Judeinstein and Sanchez, 1996). Hybrid materials obtained from sol-gel processes exhibit novel resulting properties of organic-inorganic components at the nanometer scale. Due to the above-mentioned features, these materials are regarded as highly innovative and advanced. Consequently, they hold promising applications in various fields such as optics, electronics, mechanics, functional and protective coatings, optical chemical sensors, catalysts, membranes, biology and medicine (Ogoshi and Chujo, 2005)(Sanchez et al., 2011).

2.1.3 Applications of hybrid materials

As described above, hybrid materials offer various and unique combinations of properties that make them suitable for a wide range of applications. Due to diverse application range these materials can adress many challenges. The most interesting and widely studied topics are described below.

Optoelectronics and sensors

It is widely agreed among the scientific community that hybrid materials have

a great potential for active optical applications, making it an attractive field for research. The progression of photoactive coatings and systems is an emerging field (Sanchez et al., 2011). Recent studies have reported hybrid materials having particular properties causing a better laser action and that by incorporating the specific hybrid materials can lead to enhanced photostability properties (Jiangying et al., 2018), rapid photochromic response and highly stable second-order non-linear optical response (Escribano et al., 2007), and innovative applications as pH sensors (Ren et al., 2021), electroluminescent diodes or hybrid liquid crystals (Carlos et al., 2007). APTES is one of the most often used organosilane precursor as a coupling agent for sensors.

Protective coatings

Due to many desirable properties including high transparency, good adhesion, corrosion protection and the ability to easily tune both the refractive index and mechanical properties, hybrid materials find potential utilization for a protective coatings. These coatings have found an important industrial use in such areas as optical absorption. These prepared structures often contain APTES organosilane (Carlos et al., 2007).

Catalysis

Catalysis plays a crucial role in everydays life, for example the production of energy and fuels, fine and commodity chemicals and pharmaceuticals. Hybrid materials have been explored as potential catalysts for various heterogeneous catalysis reactions. In fact, approximately 90 % of chemical manufacturing processes and over 20 % of all industrial processes rely on catalytic reactions (Hüsing, 2007). There are many forms of hybrid catalysts such as functionalized (nano)fibres, nanocoatings or nanoparticles. However, fibres are the most used in catalytic applications. Many literature sources describe organic fibres functionalized via different types of organo-mono-silylated precursors (Makova, Holubova, Krabicova, et al., 2021). Nanoparticles are for example silica-based gold- and palladium-supported (Croissant et al., 2016).

Biology and medicine

Hybrid fibrous materials made of organo-mono-silylated precursors have found a wide range of applications in the field of medicine, specifically in the development of scaffolds for cell growth and wound care. These materials are often used in combination with organic polymers and alkoxides. Hybrid fibres are for example used in bone tissue regeneration - for skeletal defect regeneration, for encapsulating bioactive molecules and maintaining their structure and function, in drug delivery systems for example working on different pH levels, for cellulose nanofibres modified via APTES to increase the mechanical properties of prepared scaffolds, for supporting a cell growth and last but not least for wound-healing applications with antibacterial effects (Makova, Holubova, Krabicova, et al., 2021).

2.2 Organosilanes

Monomeric silicon comppounds are known as silanes. A silane that contains at least one carbon-silicon bond (Si-C) structure is known as an organo-mono-silylated precursor. If there are two of carbon-silicon bonds then these are called organo-bis-silylated precursors. According to the polycondensation reaction of hybrid materials described previously in the section 2.1.1, mono-organosilanes and bis-organosilanes can react via polycondensation reaction and form large structures called polysilsesquioxanes, see figure (2.7). The general formula for organosilane molecule looks as follow:

$$(\mathrm{X{-}R})_{\mathrm{n}}{-}\mathrm{Si}(\mathrm{OR}')_{4-\mathrm{n}}$$

where X stands for a either reactive (e.g. amino group) or non-reactive (e.g. alkyl group) non-hydrolyzable organic moiety, R is typically the alkyl chain (ethyl, propyl, etc.) and OR′ is an hydrolyzable and reactive alkoxy group (Materne et al., 2012).

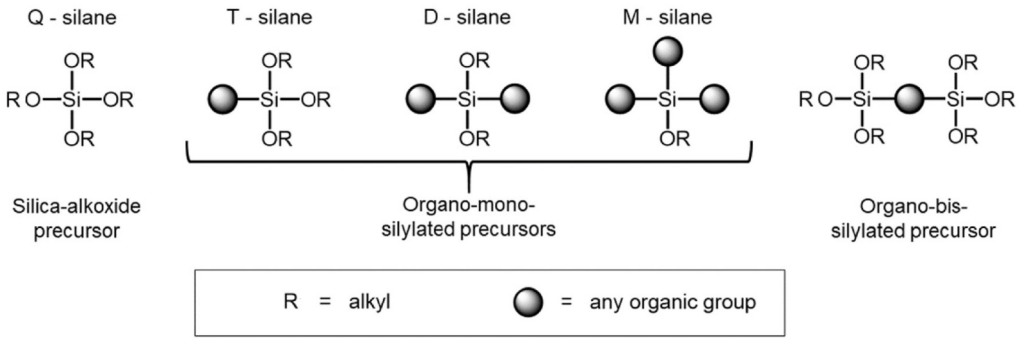

Figure 2.6: Different types of organosilanes (Makova, Holubova, Krabicova, et al., 2021).

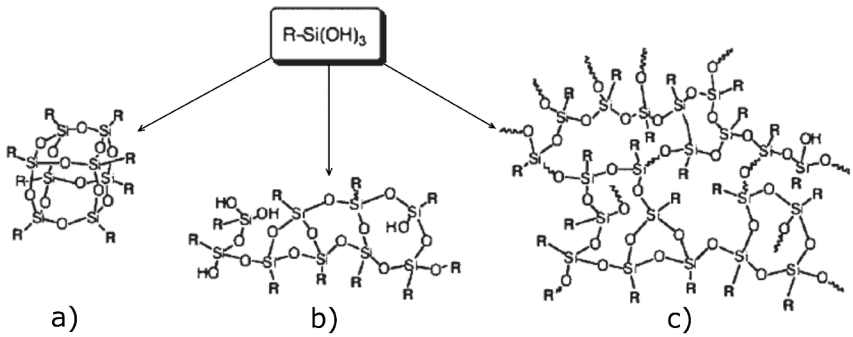

Figure 2.7: Different polysilsesquioxane structures dependent on reaction parameters - a) polyhedral oligosilsesquioxane, b) oligo and polysilsesquioxane, c) polysilsesquioxane gel (D. Loy, 2007).

Through their reactive groups connected to silica, organosilanes serve as bridges between inorganic or organic substrates (minerals, fillers, metals and cellulose) and matrices (rubber, thermoplastics or thermosets), see figure (2.8) and hence, can dramatically improve adhesion between them (Materne et al., 2012).

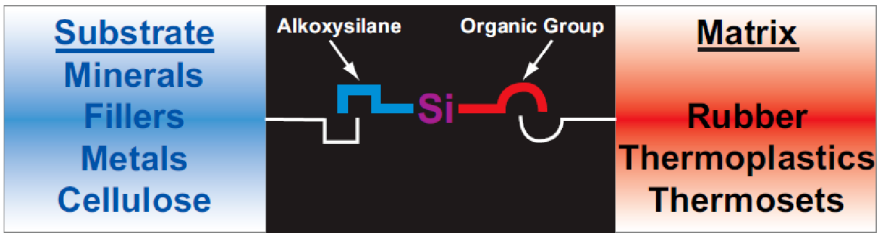

Figure 2.8: How organosilane molecules work (Materne et al., 2012)

2.2.1 Properties of organosilanes

The chemical and physical properties of organosilanes depend on the structure of organic part connected to silica. Properties that organosilane provides can be derived from its application potencial. There is a unique nature of silsesquioxanes due to the presence of the three reactive groups in the monomer and three siloxane bonds in each repeat unit. This allows silsesquixanes to form in various range of architectures, from polyhedral oligosilsesquioxanes to macromolecular bridged polysilsesquioxanes composites (D. Loy, 2007).

Porosity

Porosity is a physical property that describes the presence of empty spaces or pores in a material. These empty spaces affect the material's physical characteristics, such as the surface area or density indirectly impacting the material's melting point.

In the early 1990s, researchers introduced silica-silsesquioxane and bridged polysilsesquioxane aerogels. These aerogels have the surface areas ranging generally from 200 to 1900 m^2/g. Arylene-bridged polysilsesquioxanes are reaching the highest level of porosity and hence the highest surface areas. Silsesquioxane and polysilsesquioxanes aerogels are frequently more hydrophobic than most silica aerogels, while bridged polysilsesquioxanes are moderately hydrophilic (D. A. Loy, 2018).

According to polysilsesquioxane aerogels, there are also polysilsesquioxane xerogels having surface areas between 400 and 620 m^2/g. Bridged polysilsesquioxane xerogels typically have much higher surface areas than pendant polysilsesquioxanes or silica xerogels and specifically with rigid arylene, alkenylene, and alkynylene groups they exhibit significant micropores and mesopores, resulting in surface areas as high as 1200 m^2/g. On the other hand, bridged polysilsesquioxanes containing flexible bridging groups longer than six carbons are nonporous in acidic conditions (D. A. Loy, 2018).

Thermal stability

Thermal stability is a combination of both physical and chemical properties. Thermal stability describes the material's resistance to decompose or degrade when exposed to high temperatures. It is dependent on the material's chemical structure such as connected functional groups or bonding pattern and physical properties like melting point, heat capacity or thermal conductivity.

The thermal stability of polysilsesquioxanes can be as high as 500 °C and in fact depends on the stability of the organic group (D. Loy, 2007)(Makova, Holubova, Krabicova, et al., 2021). Polysilsesquioxanes can have different substituents and bridging groups, which affect their thermal stability. For example with aryl substituents or bridging groups can withstand high temperatures of 400-500 °C, however alkyl substituents and alkylene-bridging groups have lower stability and can only withstand temperatures up to 300-400 °C. Organosilanes containing allylic, acetylenic or alkyl linkers together with leaving groups in the form of halides, alkoxy groups or acetates located near silicon are even less stable and degrade at low temperatures (D. A. Loy, 2018).

Adhesion

Adhesion belongs to the combination of both physical (van der Waals forces) and chemical (formation of chemical bond) properties. Organosilanes are compounds that can improve the adhesion between a surface and a coating. When they are used as an additive, the organosilane must move to the interface between the substrate and the adhesive layer to be effective.

Organosilanes are mostly used for coatings that provide benefits such as improved thermal stability, UV resistance, stronger adhesion, low surface tension or flow properties. In this case they provide a barier properties that resist to many contaminants and electrolytes, due to the high crosslinking density (Materne et al., 2012).

2.2.2 Applications of organosilanes

Organo-mono-silylated precursors

Organosilanes offer effective adhesion between substrates and adhesive layers, making them useful additives or primers for paints, inks, coatings, adhesives and sealants. Their properties make them suitable for various coating applications.

By combining silanes with organic resins and carefully managing the hydrolysis/condensation balance, coatings with superior properties can be achieved. Chemistries such as siloxane-epoxy and siloxane-acrylic significantly enhance industrial, architectural and marine antifouling coatings (Materne et al., 2012).

Incorporating organosilanes with hydrophobic organic groups into hydrophilic inorganic surfaces imparts hydrophobicity, making them durable hydrophobing agents for use in various concrete construction applications, such as bridge and deck constructions (Materne et al., 2012).

Organosilanes are also used as water scavengers in moisture-sensitive formulations, blocking agents in antibiotic synthesis and silicate stabilizers. While silica-based materials are biocompatible and suitable for use *in vivo*, the safety of organo-bridged materials remains uncertain due to limited research (Makova, Holubova, Krabicova, et al., 2021).

Organo-bis-silylated precursors

Hybrid organosilane materials based on organo-bis-silylated precursors, mainly nanoparticles, appear to be a promising class of materials with exceptional properties applicable in separation methods, such as chromatographies. Organo-bis-silylated precursors containing organic aromatic rings provide properties like electrical conductivity. They are also promising candidates for optoelectronics, sensing devices or energy storage (Makova, Holubova, Krabicova, et al., 2021).

The incorporation of organic molecules into the resulting materials influences the mechanical, chemical and/ or thermal stability of these materials.

Organo-bis-silylated polysilsesquioxanes functionalized with amino and thiol groups have also been utilized as adsorbents of volatile organic compounds from gas phase chromatography. Polysilsesquioxanes bridged with arylene exhibit unique characteristics such as high surface area and porosity, which make them suitable for filtration, catalysis and adsorption. Arylene bridged polysilsesquioxane fibres exhibit the same properties (Makova, Holubova, Krabicova, et al., 2021).

As mentioned above, the real value of organo-bis-silylated polysilsesquioxanes is in their utility for preparing highly functionalized gels. For example, porous xerogels of thiourea-bridged polysilsesquioxanes have been shown to be effective in recovering transition metals from water. Polysilsesquioxane xerogels can hold organic and organometallic dyes or inorganic quantum dots for photonics applications (D. Loy, 2007).

2.2.3 Reactions of organosilanes

There exists a three pathways how to obtain porous organosilane hybrid materials that are described in *Silica-Based Mesoporous Organic–Inorganic Hybrid Materials* (Hoffmann et al., 2006):

1. the subsequent modification of the pore surface of a purely inorganic silica material (“grafting”)

2. the simultaneous condensation of corresponding silica and organosilica precursors ("co-condensation")

3. the incorporation of organic groups as bridging components directly and specifically into the pore walls by the use of bis-silylated single-source organosilica precursors ("production of periodic mesoporous organosilicas")

Grafting

The process of grafting involves modifying the inner surfaces of mesostructured silica phases with organic groups. This is achieved by reacting organosilanes, chlorosilanes or silazanes with the free silanol groups of the pore surfaces. The advantage of this method is that it usually retains the mesostructure of the starting silica phase while reducing the porosity of the hybrid material. However, if the organosilanes react mainly at the pore openings during the initial stages of the process, the diffusion of further molecules into the centre of the pores can be impaired, leading to a non-homogeneous distribution of organic groups. For some cases, bulky grafting species can even result in the complete closure of the pores, known as pore blocking (Hoffmann et al., 2006).

Co-condensation

In addition to grafting, a one-pot synthesis method called co-condensation has been developed for synthesising organically functionalized mesoporous silica phases. This method involves the co-condensation of tetraalkoxysilanes (TEOS) and terminal trialkoxyorganosilanes in the presence of structure-directing agents. The resulting material has organic residues covalently anchored to the pore walls and projecting into the pores, while the organic functionalities are integrated as direct components of the silica matrix. This method offers several advantages, including the absence of pore blocking and more homogeneous distribution of the organic units compared to grafting.

Sol-gel reaction of organosilanes

Organosilanes can easily hydrolyse and condense and this property is typically used in sol-gel reaction. Organo-mono-silylated or bridged organo-bis-silylated monomers react with water in the presence of acid/base catalyst. Environment for the reaction is chosen according to solubility of monomers and to ensure a homogeneous solution for polymerisation. Solvents such as alcohol play a crucial role in particle nucleation and gelation. Silanols are formed during the sol-gel reaction when the alkoxide groups undergo hydrolysis and condense to the form of Si-O-Si linkages. Firstly are produced oligosilsesquixanes and then polysilsesquioxanes (D. Loy, 2007).

The sol-gel polymerisation process can result in the formation of particles, coatings, or gels, depending on the conditions used. Particles can be form through precip-

itation or suspension in the sol, while coatings can be applied through methods such as dip-coating, spin-coating, or spraying. Gels can be dried in different ways - air-drying to form monolithic xerogels and supercritical drying to produce monolithic aerogels (D. Loy, 2007).

2.3 Fibre formation techniques

Electrospinning is a widely utilized technique for producing ultra-thin fibres made of polymeric, metal oxide materials, and their composites. The technique has undergone considerable advancements in terms of electrospinning methodology and engineering of electrospun nanofibres to suit various applications. However, the production stage of electrospun nanofibres faces several challenges, including large volume processing, reproducibility, and safety concerns (Makova, Holubova, Krabicova, et al., 2021).

The electrospinning process involves four key components: a high-voltage power supply, a syringe pump, a spinneret and a collector. A small amount of viscoelastic fluid is pumped through the spinneret and the resulting spherical droplet is quickly charged by the high-voltage. This causes repulsion among the charges, deforming the droplet into a conical shape and creating a jet that forms fibres as it passes through the air and solvent evaporation occurs. The electrospinning process is affected by several variables, including environmental parameters (e.g. solution temperature, humidity, and air velocity in the electrospinning chamber), solution properties (e.g. elasticity, viscosity, conductivity, and surface tension), and governing variables (e.g. distance between the tip and counter electrode, electrical potential, flow rate, molecular weight of the selected polymers, and collector geometry). One of the critical factors influencing fibre formation is the viscosity of the spinning solution. To achieve micro to nanoscale diameter fibres, we need to adjust the viscosity of polymer solution (e.g. evaporating of the solvent) (Makova, Holubova, Krabicova, et al., 2021).

However there are other fibre-making techniques, showed in the figure (2.9), such as drawing or self-assembly. Drawing method involves the mechanical pulling of a polymer solution out of its base droplet, resulting in fibre solidification, while solvent evaporates. Drawing can be performed with glass micro-pipettes, atomic force microscope or scanning tunneling microscope probe tips. Drawing process has some disadvantages, such as limited process control, limited-time influenced by droplet solidification, changes in droplet viscosity, and solvent evaporation speed, however between its advantages belong producing oriented fibres ranging from nanometers to micrometers, unlike electrospun fibres that are randomly oriented (Makova, Holubova, Krabicova, et al., 2021).

Self-assembly is a process in which pre-existing components such as molecules, polymers, or particles spontaneously organize into ordered structures or patterns

without external direction. This process is driven by energy minimization and thermodynamic equilibrium, resulting in various shapes and forms. Manipulating these fibres is also challenging, as they cannot form a continuous layer within a solution, compared to electrospun fibres (Makova, Holubova, Krabicova, et al., 2021).

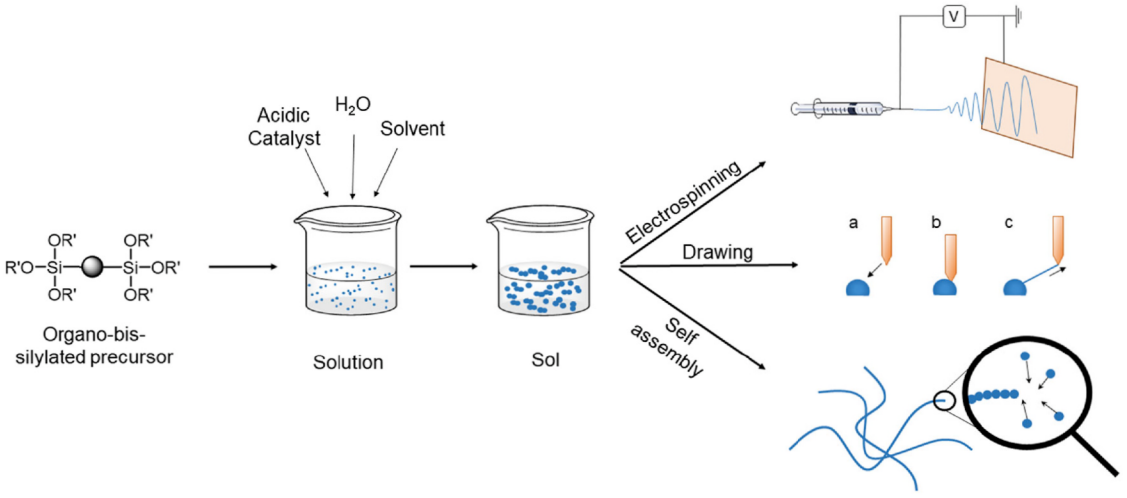

Figure 2.9: Preparation of nanofibres from organo-bis-silylated precursors using various fibre making techniques (Makova, Holubova, Krabicova, et al., 2021).

3 Experimental part

Chemicals and solvents used were purchased from Tokyo Chemical Industry CO., LTD., Ing. Petr Švec – PENTA s.r.o., Sigma-Aldrich s.r.o., Lach-Ner, s.r.o. and Gelest, Inc.

^{1}H-NMR including 2D ^{1}H NMR and ^{13}C NMR spectra were measured by Christopher James Hobbs, PhD with JNM-ECZ400R/M1, JEOL. Mass spectrometry was measured by MSc. Vít Novotný with ICP-MS. FTIR spectra were measured by MSc. Martin Stuchlík and MSc. Jana Müllerová, PhD with Nicolet iZ10, Thermo Scientific, USA. TGA was measured by MSc. Martin Stuchlík with TGA Q500, TA Instruments, USA. Viscosity of samples was measured with vibration viscometer SV-1A, A&D Scientech. Pictures of the fibres were taken by MSc. Johana Kulhánková and measured with scanning electron microscope Tescan Vega 3.

Synthesis of the precursor containing oxalyl organic part is based on the article (Fatieiev et al., 2015). Syntheses in this thesis are developed and modified for the best results and post-processing of final material.

In this thesis is followed the given patent that Assoc. Prof., MSc. Veronika Máková, PhD and her colleagues published: *Method for the preparation of a sol for the preparation of hybrid organosilane fibres be electrostatic spinning, the sol prepared by this method and hybrid organosilane fibres prepared by the electrostatic spinning of this sol* (Makova, Holubova, and Kulhankova, 2022).

3.1 General synthetic procedure

Unless stated otherwise, all precursors were prepared using the common procedure as follows. All necessary information for synthetic procedures are included in the table (3.1). A round bottom flask was dryed over night (100 °C) and was kept under argon for reaction. Dry solvent was mixed with organic component in the flask, stirred at 500 rpm at 0°C using an ice bath. After dissolving, TEA was added to the reaction flask. Finally, organosilane was added dropwise and the reaction mixture was left mixing for 4 hours at RT.

The solution was washed with dH_2O using separation funnel. This step was repeated 3 times. Washed organic component (product) was obtained over $MgSO_4$. Remaining toluene was removed using a rotovap at 20 mBar/50 °C. Product was then redissolved in dry toluene and evaporated once again. The product was redissolved again in dry toluene and $MgSO_4$ removed using either a vacuum filtration (with S3 porosity filter) or centrifugation (12,000 rcf/30 minutes). Finally the product was filtered with a 0.22 µm syringe filter and toluene removed in a rotovap before final drying at 0 mbar/75 °C/8 hours. Yield was measured.

Obtained product was subjected to several characterisation methods mentioned above. For further analysis, ^{1}H NMR, ^{13}C NMR and MS were neccessary.

The BTPO precursor was synthesised using small variations according to general synthesis procedure. The dry solvent was first mixed with organosilane, while preparing a diluted organic component in 30 ml DCM. When TEA was added, the diluted organic component was added dropwise into the reaction mixture.

Table 3.1: Chemicals and their amounts, separation methods and yields of all synthesised precursors.

Synthesised precursors	Solvent for initial reaction		Organic component		TEA	Organo-mono-silane	
BiTSAP	Toluene	200 ml	PDC	5.33 g, 26.14 mmoles	10.93 ml, 78.42 mmoles	APTES	12.23 ml, 52.28 mmoles
BTPO	DCM	250 ml	$COCl_2$	4.29 ml, 50.02 mmoles	20 ml, 150.66 mmoles	APTES	23.63 ml, 100.97 mmoles
BiTSAB-a	Toluene	200 ml	TPC	5.31 g, 26.18 mmoles	10.95 ml, 78.55 mmoles	APTES	12.26 ml, 52.37 mmoles
BiTSAB-b	Toluene	250 ml	TPC	4.75 g, 23.4 mmoles	9.78 ml, 70.2 mmoles	APMDES	9.78 ml, 46.8 mmoles
BiTSAB-c	Toluene	10 ml	TPC	0.31 g, 1.54 mmoles	0.65 ml, 4.65 mmoles	APDMES	0.58 ml, 3.1 mmoles

Synthesised precursor	Solvent for washing				$MgSO_4$	Separation method	Yield [%]
BiTSAP	dH2O	200 ml	Toluene	200 ml	0.5 g	Filtration	92.65
BTPO		100 ml	DCM	150 ml	1 g	Filtration	61.42
BiTSAB-a		200 ml	Toluene	100 ml	0.5 g	Filtration	93.82
BiTSAB-b		200 ml	Toluene	100 ml	0.5 g	Filtration	87.14
BiTSAB-c		15 ml	Toluene	20 ml	0.3 g	Centrifuge	65.69

3.2 General procedures for method sol-gel and fibres formation

Unless stated otherwise, all sol-gel reactions were undertaken with the common proceedure as follows. All necessary information are included in the table (3.2). A round bottom flask was dryed over night (100 °C), the product was weighed into the flask, dissolved in ethanol and put on magnetic stirrer. A condenser with water cooling was put on round bottom flask. The prepared mixture of water and HCl was then added, when the product was fully dissloved. The flask was left mixing.

The reaction was interrupted with the destillation step. Finally, a condenser was put on the round bottom flask to distil and adjust the amount of solvent in the final sol. The magnetic stirrer was set to 600 rpm/78 °C. Viscosity was checked before proceeding on electrospinning.

Table 3.2: Chemicals, their amount and parameters of sol-gel reaction.

Synthesised precursor	Amount	Ethanol	demiH_2O	HCl	Magnetic stirrer	Time
BiTSAP	19.274 g	96.4 ml	752 µl	347 µl	350 rpm/90 °C	1 h
BTPO	17.03 g	95 ml	800 µl	240 µl	350 rpm/60 °C	6 days
BiTSAB-a	2 g	15 ml	68 µl	7 µl	500 rpm/75 °C	72 h
BiTSAB-b	2 g	15 ml	5 µl	7 µl	400 rpm/75 °C	72 h
BiTSAB-c	0.441 g	4.5 ml	5 µl	6 µl	400 rpm/75 °C	24 h

BiTSAP and BTPO precursors were proceed using Nanospider electrospinning device by MSc. Johana Kulhánková, while the BiTSAB-a, BiTSAB-b and BiTSAB-c were proceed using needle electrospinning. Thus there are two tables below showing the electrospinning parameters.

Table 3.3: Needle electrospinning parameters.

Synthesised precursor	Distance electrode/collector	Voltage	Syringe pump speed	Viscosity
BiTSAB-a	20 cm	27 kV	24.5 ml/hr	140 mPa.s
BiTSAB-b	20 cm	30 kV	3 ml/hr	38.9 mPa.s
BiTSAB-c	20 cm	24 kV	5 ml/hr	_

Table 3.4: Nanospider electrospinning parameters.

Synthesised precursor	Distance electrode/collector	Voltage [kV]	
		Electrode	Collector
BiTSAP	16 cm	40	-20
BTPO	16 cm	40	-20

Synthesised precursor	Speed of cartridge	Temperature	Humidity
BiTSAP	300 mm/s	22	30
BTPO	340 mm/s	24	28

figures (3.1 - 3.5) show the final structure of synthesised precursors using general synthetic procedure.

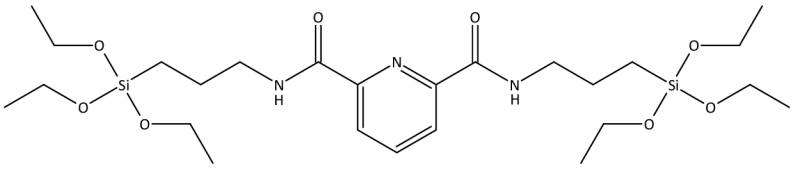

Figure 3.1: *N,N′*-bis(3-(triethoxysilyl)propyl)pyridine-2,6-dicarboxyamide (BiTSAP).

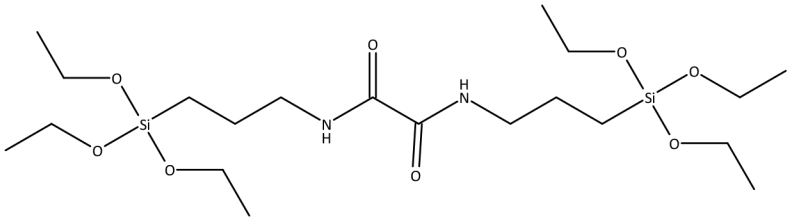

Figure 3.2: *N,N′*-bis(3-(triethoxysilyl)propyl)ethanediamide (BTPO).

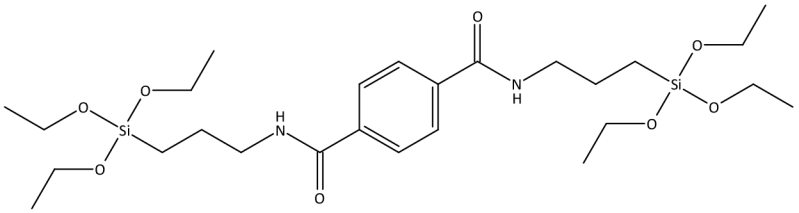

Figure 3.3: *N,N′*-bis(3-(triethoxysilyl)propyl)benzene-1,4-dicarboxyamide (BiTSAB-a).

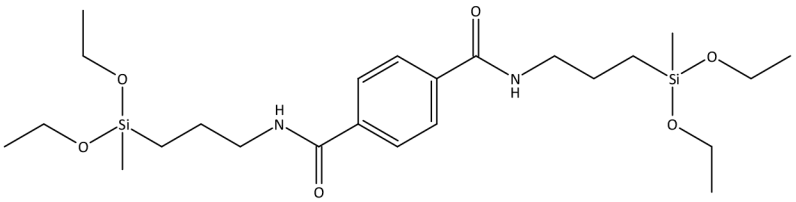

Figure 3.4: *N,N′*-bis(3-(diethoxy(methyl)silyl)propyl)benzen-1,4-dicarboxyamide (BiTSAB-b).

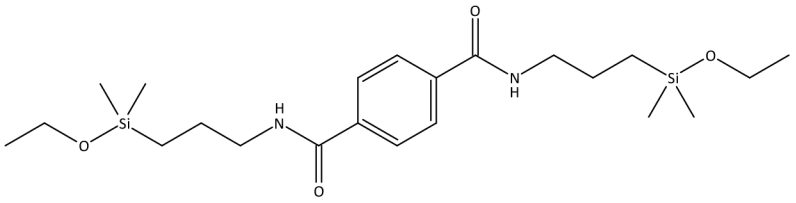

Figure 3.5: *N,N′*-bis(3-(ethoxydimethylsilyl)propyl)benzen-1,4-dicarboxyamide (BiTSAB-c).

4 Results and discussion

4.1 General Characterisation of synthesised compounds and (nano)fibres

4.1.1 Liquid state (LS) NMR

The structures of the precursors were confirmed using 1D and 2D LS NMR spectrometry. ^{1}H NMR spectra displayed peaks which were assigned based on relative position and chemical shifts in conjunction with the relative integrals and peak splitting, and further identified through 2D COSY spectra. ^{13}C NMR spectra were assigned from the relative chemical shifts. In general, the spectra obtained were used to confirm the structure and observing any potential contaminants, by-products, or residual solvent.

4.1.2 Mass spectrometry

The mass (mass/charge) of the expected synthesised compounds was calculated using the ChemDraw software. Analysis of all observed signals confirmed that no other species of organosilanes and/or by-products were present in the prepared precurors. All synthesised precursors were found with predominantly the H^{+} and Na^{+} ions.

4.1.3 FTIR

Obtained FTIR spectra display peaks which provide information about the specific bonds present in the prepared precursor. FTIR spectra was primarily measured to observe the presence of the formed amide bond in the synthesised precursor. In addition, comparisons between the pure precursors and formed fibres were analysed.

4.1.4 Solid-state (SS) NMR

Solid-state NMR was used to observe ^{13}C and ^{29}Si from the formed fibres. ^{13}C was assigned using information from the LS ^{1}H spectra. The ^{29}Si spectra was assigned based on the modes of condensation (as depicted in figure 2.6, able to observe M, D, T, or Q units). For all obtained spectra, the relative integrals were obtained

(from direct-pulse excitation) from a deconvoluted spectra, which was used to determine the remaining (unreacted) ethoxy units present in the fibres. Furthermore, the deconvolution of the obtained ^{29}Si spectra allows the determination of the degree of polycondensation, which was shown to be in agreement with the calculated ethoxy units (^{13}C spectra).

4.2 *N,N′*-bis(3-(triethoxysilyl)propyl)benzene-1,4-dicarboxyamide

4.2.1 Characterisation of the precursor

NMR

In the figure (4.1) we can see liquid state ^{1}H and ^{13}C NMR, where hydrogens are labeled with red letters and carbons labeled with blue numbers. Furthermore splitting shapes of the peaks are shown, providing valuable information for confirmation of the synthesised precursor structure (n+1 rule). We can see that synthesised product is in general pure (no unexpected carbons or hydrogens present in spectra).

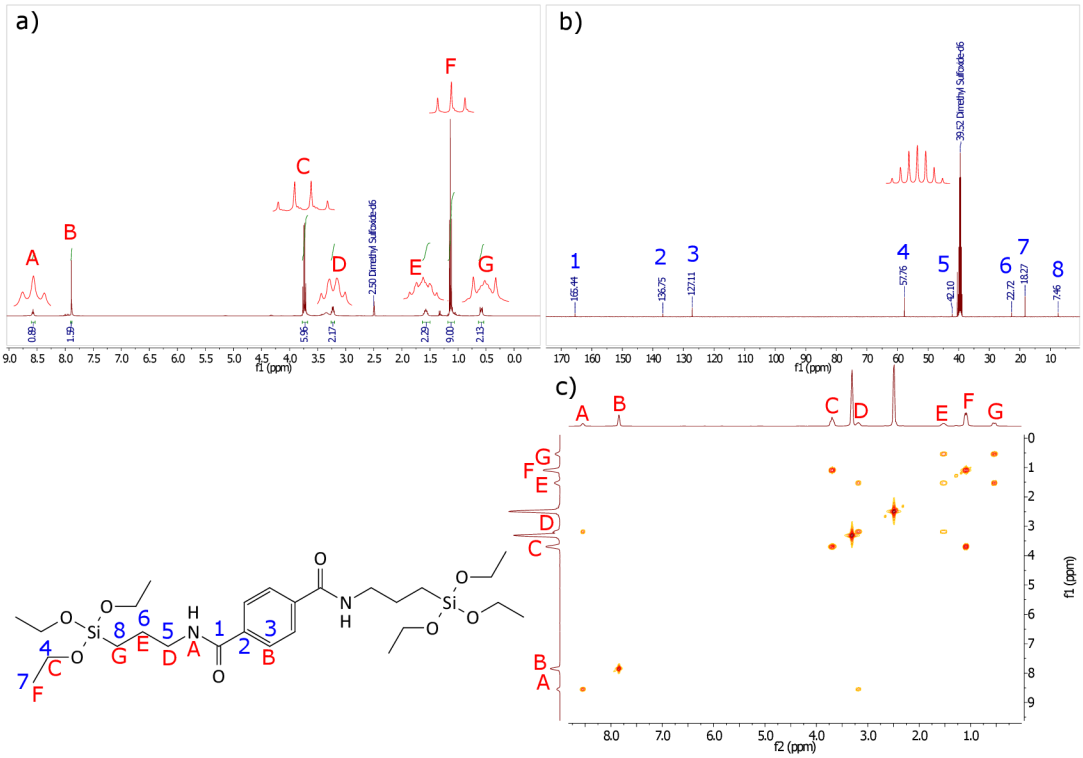

Figure 4.1: a) ^{1}H NMR, b) ^{13}C and c) 2D COSY NMR of BiTSAB-a.

Mass spectrometry

In figure (4.2), the main masses observed are at 574.297 and 596.278. For the

BiTSAB-a precursor, the theoretical mass (m/z) is 573.30. Therefore, the observed masses align well with the expected structure mass, whereby the predominant m/z found in the figure is the product with H^+ or Na^+.

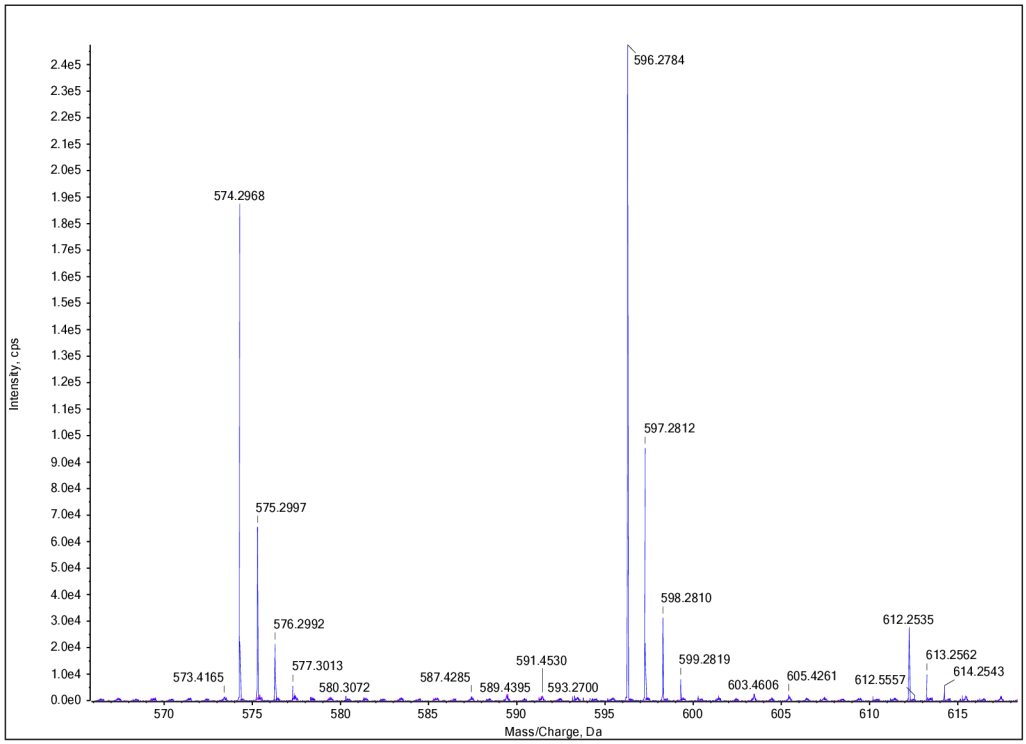

Figure 4.2: MS of BiTSAB-a.

FTIR

In figure (4.3) we can see at 3309 cm^{-1} water, Si−OH and −NH bonds present. At 2972 cm^{-1} we can see aliphatic carbon chain bonds $-CH_2-$ and $-CH_3$. At 1632 and 1543 cm^{-1} we can see amide peaks that provide information about carbonyl and amide bonds. Around 1000 cm^{-1} are various types of silica bonds shown.

TGA

TGA provides information about thermal stability of the prepared precursor, which start decomposing at 121.34 °C (4.4).

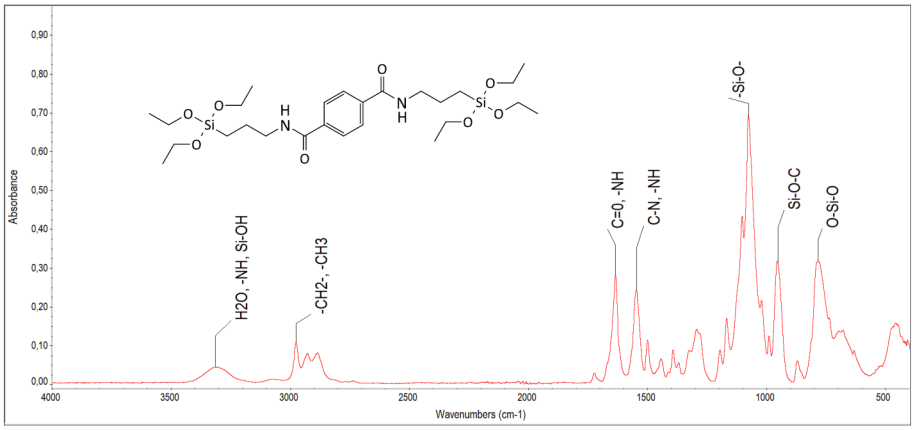

Figure 4.3: FTIR of BiTSAB-a.

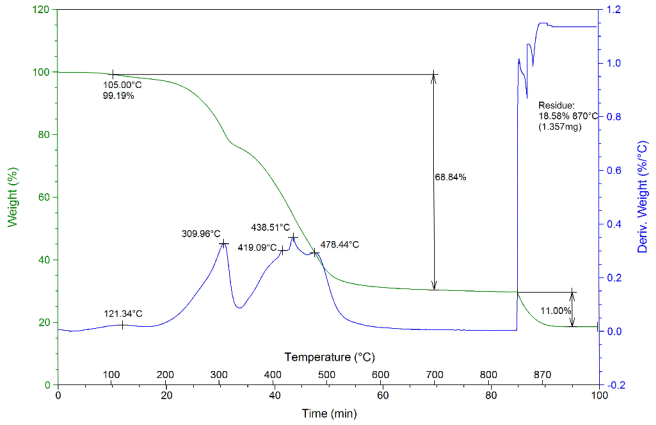

Figure 4.4: TGA of BiTSAB-a.

4.2.2 Characterisation of the prepared fibres

SEM

SEM method give us information about fibres appearance, their possible defects and size distribution. The fibres in the figure (4.5) are in general homogenous, smooth and rounded without visible defects. Measuring 100 fibres results in an average diameter of 2.6 µm for the formed fibres.

TGA of fibres

As shown below (4.6), the fibres exhibit higher thermal stability in comparison to precursor (4.4). While precursor started decomposing at 121 °C, fibres started decomposing at 359 °C.

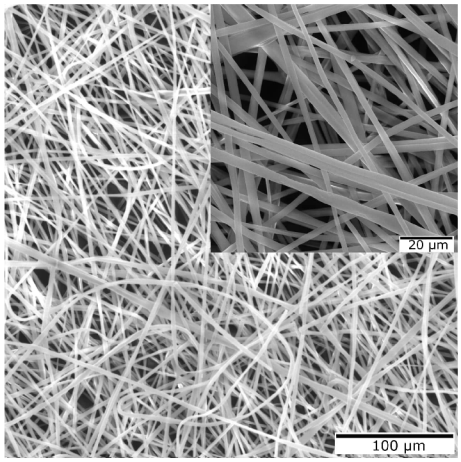

Figure 4.5: SEM of BiTSAB-a fibres.

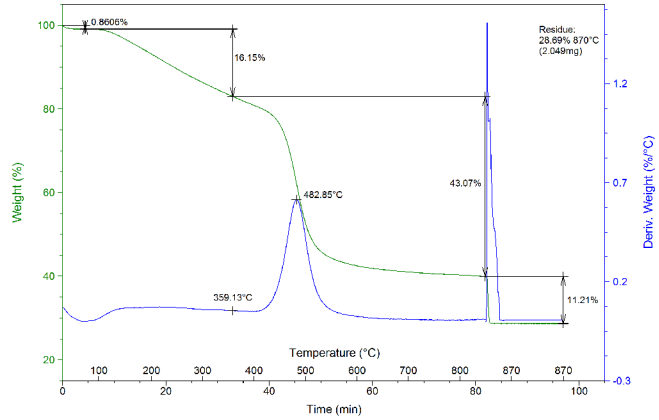

Figure 4.6: TGA of BiTSAB-a fibres

NMR of fibres

Fibres were subjected to solid state NMR which provides valuable information for the formed fibres such as the degree of polycondensation. From calculations using NMR spectral data, the degree of polycondensation was determined to be 46 %, with 41 % remaining ethoxy groups present and thus 13 % are OH groups. R in the figure of the molecule depicts the potential structure consisting of O−Si or $O-CH_2CH_3$ or −OH.

FTIR of fibres

Figure (4.8) shows the comparison of the precursor and the fibres, measured by FTIR spectroscopy. We can see that main structure remained the same, but the peak around 1000 cm^{-1} got broader, this is due to growth of Si-O-Si inorganic chain.

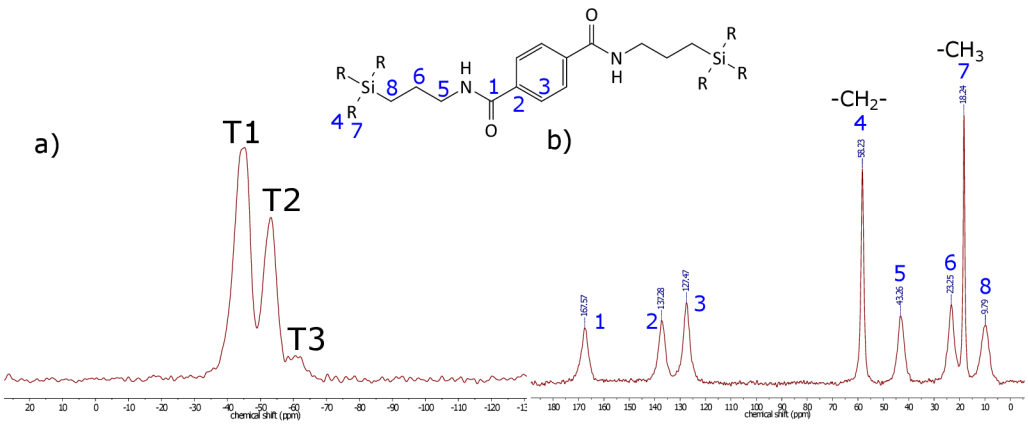

Figure 4.7: a) ^{29}Si and b) ^{13}C NMR of BiTSAB-a fibres.

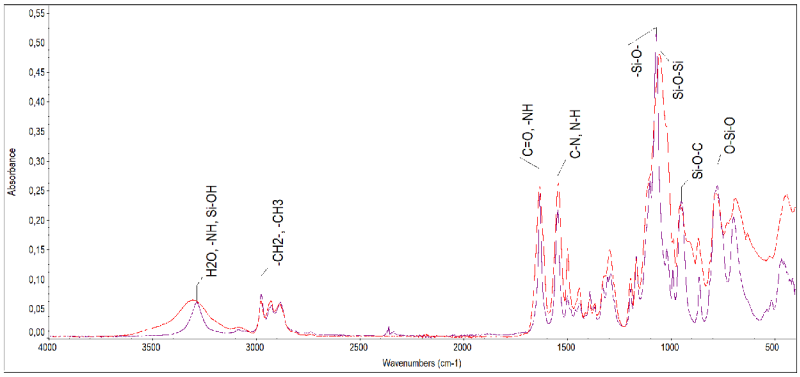

Figure 4.8: FTIR of BiTSAB-a fibres.

4.3 *N,N′*-bis(3-(triethoxysilyl)propyl)pyridine-2,6-dicarboxyamide

4.3.1 Characterisation of the precursor

NMR

In the figure (4.9) we can see liquid state ^{1}H and ^{13}C NMR. We can see that synthesised product is in general pure (no presence of unexpected carbons or hydrogens in the spectra).

Mass spectrometry

In figure (4.10), the main masses observed are at 574.296 and 596.279. For the BiTSAP precursor, the theoretical mass (m/z) is 573.29. Therefore, the observed masses align well with the expected structure mass, whereby the predominant m/z found in the figure is the product with H^+ or Na^+.

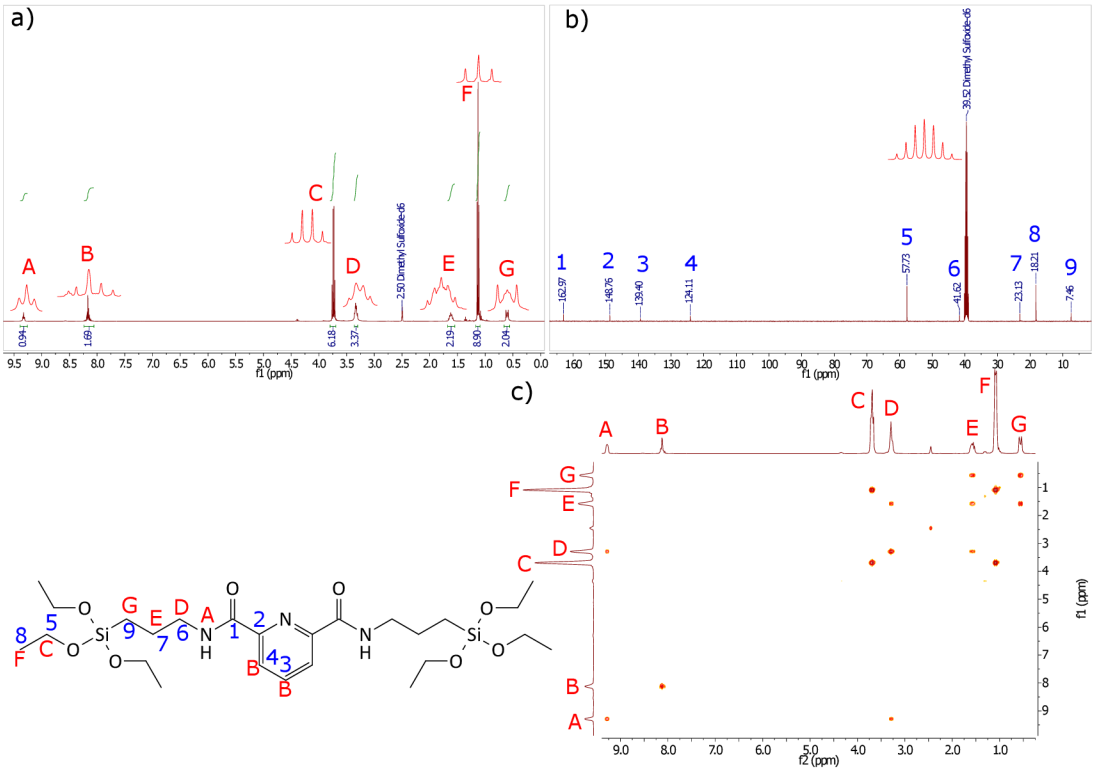

Figure 4.9: ^{1}H, ^{13}C and 2D COSY NMR of BiTSAP.

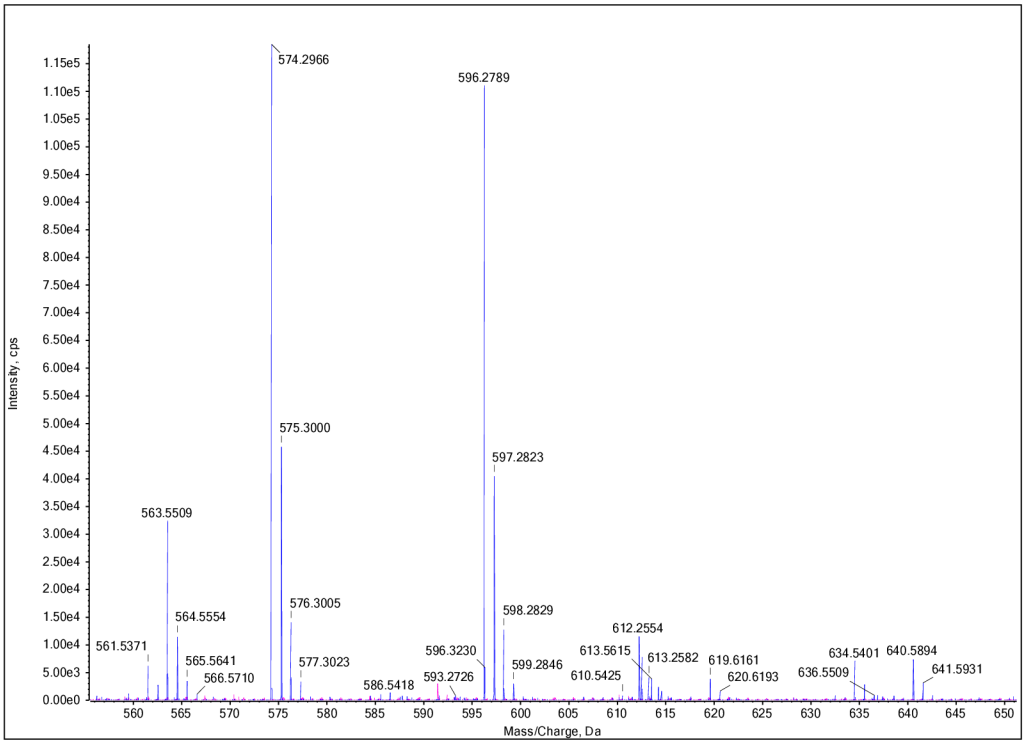

Figure 4.10: MS of BiTSAP.

FTIR

In figure (4.3) we can see at 3309 cm^{-1} water, $Si-OH$ and $-NH$ bonds present. At 2972 cm^{-1} we can see aliphatic carbon chain bonds $-CH_2-$ and $-CH_3$. At 1632 and 1543 cm^{-1} we can see amide peaks that provide information about carbonyl and amide bonds. Around 1000 cm^{-1} are various types of silica bonds shown.

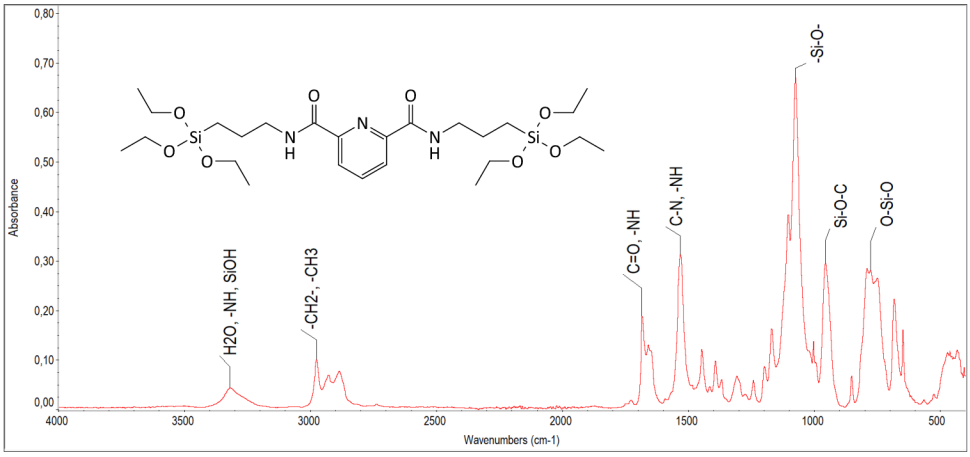

Figure 4.11: FTIR of BiTSAP.

TGA

In the figure (4.12) we can see, that measured sample started decomposing at 128.53 °C.

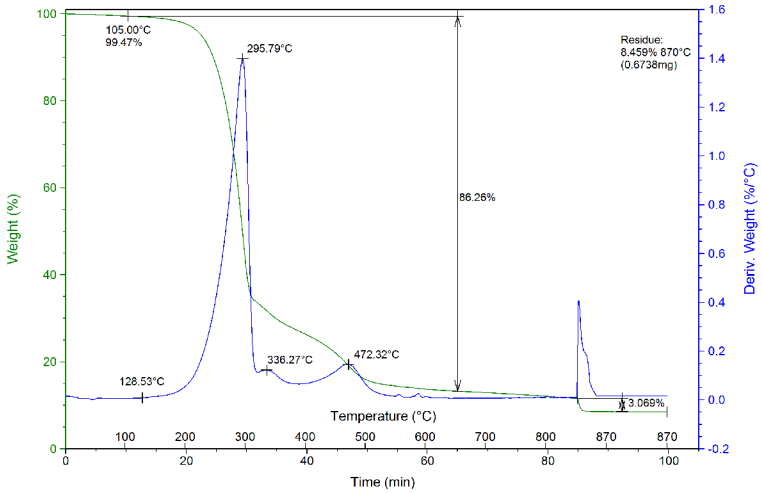

Figure 4.12: TGA of BiTSAP.

4.3.2 Characterisation of the prepared fibres

SEM

In the figure (4.13) we can see thinner distributed fibres in comparison to the BiTSAB-a or BiTSAB-c. This can be due to use of a different electrospinning technique. The fibres look in general homogenous, smooth and without any visible defects. The size of the fibres was measured on 100 fibres and on average is 1 µm.

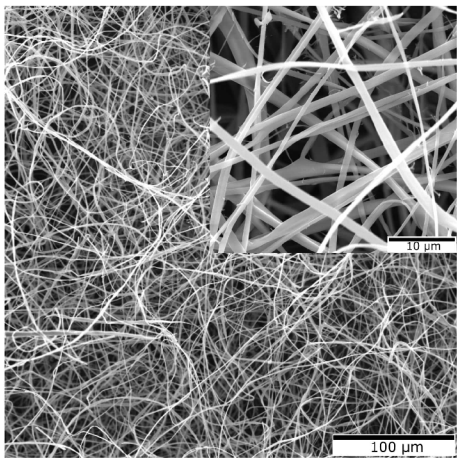

Figure 4.13: SEM of BiTSAP fibres.

There were no further fibre analysis of BiTSAP made due to a lack of the time and due to problems using measuring devices.

4.4 *N,N′*-bis(3-(triethoxysilyl)propyl)ethanediamide

4.4.1 Characterisation of the precursor

NMR

In the figure (4.9) we can see liquid state ^{1}H and ^{13}C NMR. We can see that synthesised product is pure, however the is a presence of water in the product. Water (3.3 ppm peak) probably remained with the product from washing steps or there could be appearance of the water in the solvent used for NMR analysis.

Mass spectrometry

In figure (4.15), the main masses observed are at 497.271 and 519.252. For the BTPO precursor, the theoretical mass (m/z) is 496.26. Therefore, the observed masses align well with the expected structure mass, whereby the predominant m/z found in the figure is the product with H^{+} or Na^{+}.

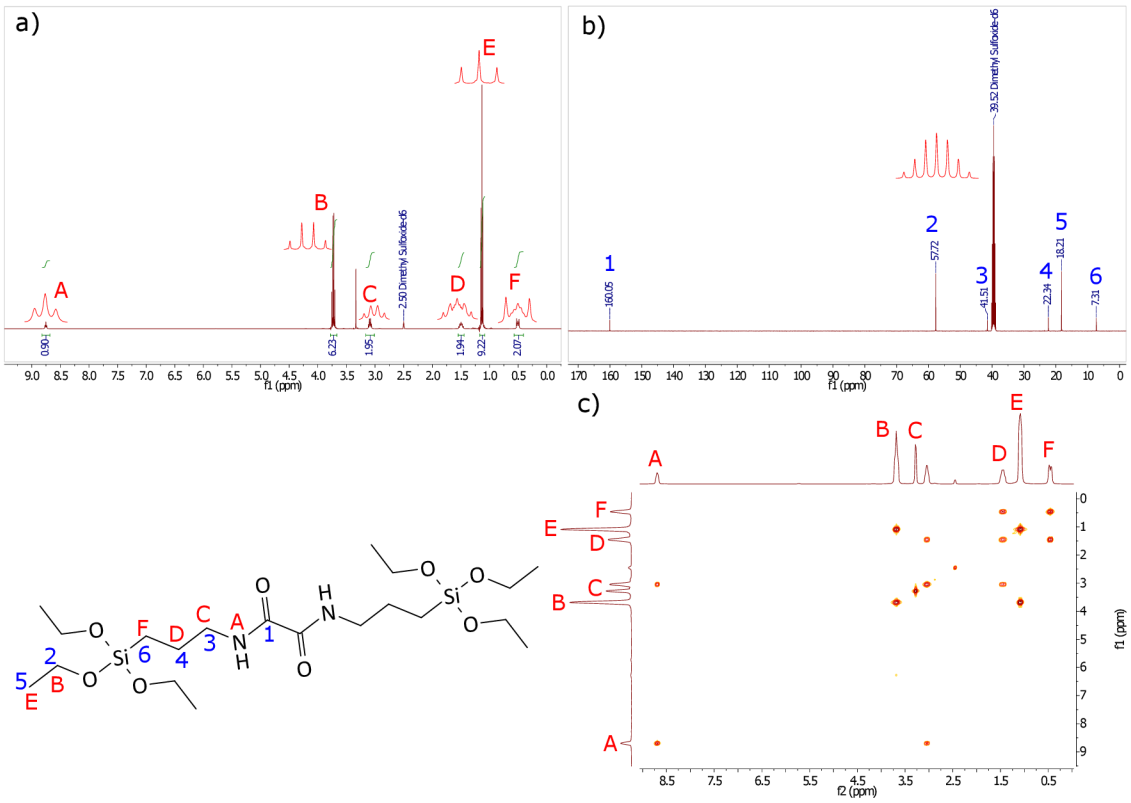

Figure 4.14: ^{1}H, ^{13}C and 2D COSY NMR of *N,N′*-bis(3-(triethoxysilyl) propyl)ethanediamide

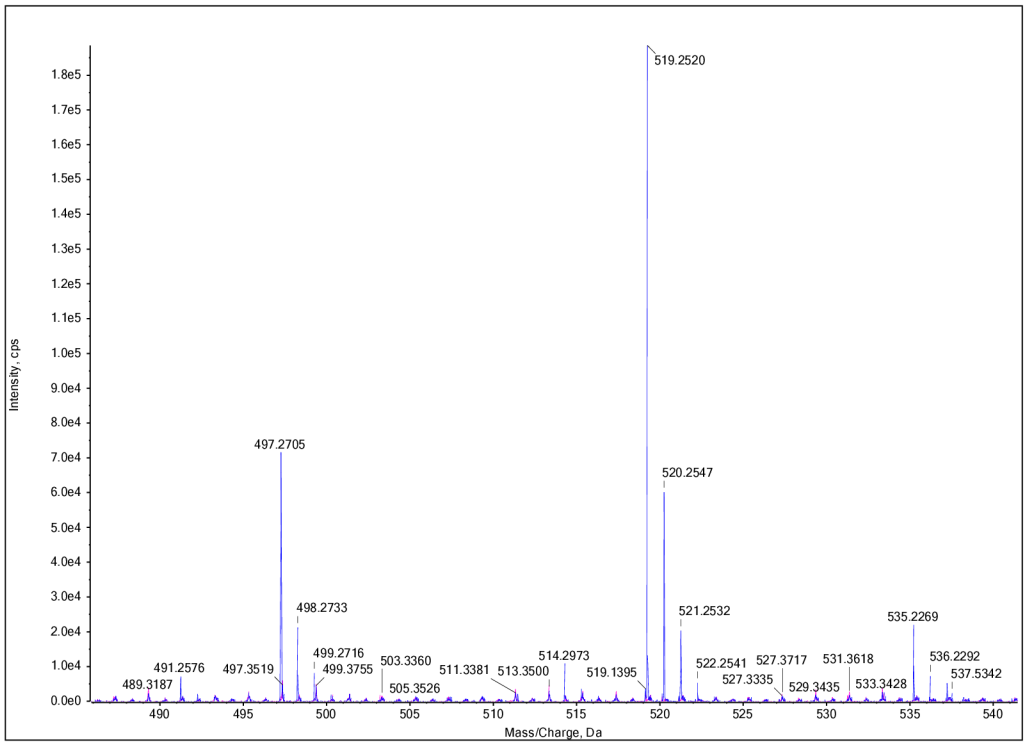

Figure 4.15: MS of BTPO

FTIR

In the figure below (4.16) we can see water, Si−OH and −NH bonds around 3300 cm^{-1} present. Around 3000 cm^{-1} we can see aliphatic carbon chains $-CH_2-$ and $-CH_3$. Around 1700 to 1500 we can see peaks providing information about carbonyl and amide bonds. Around 1000 cm^{-1} are various types of silica bonds shown.

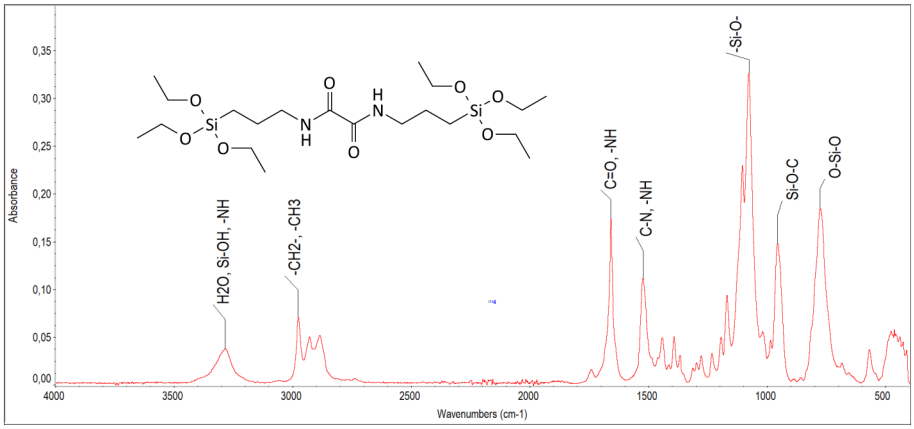

Figure 4.16: FTIR of BTPO

TGA

In the figure (4.17) we can't see the exact temperature of the start of the precursor decomposition, however approximately the temperature equals ≈ 130 °C.

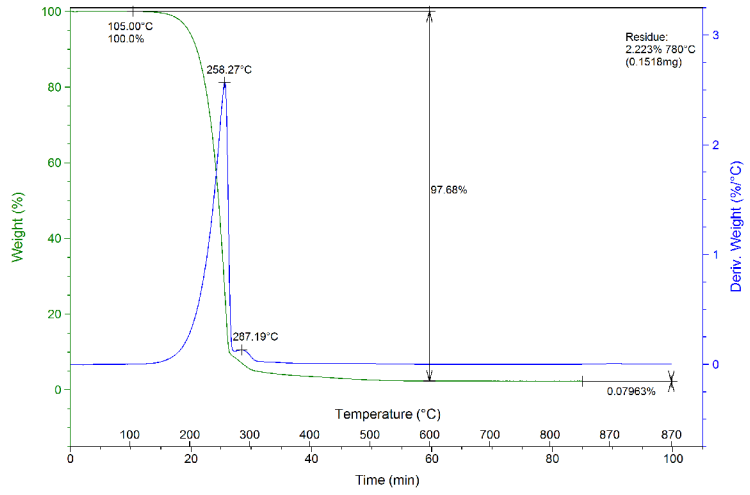

Figure 4.17: TGA of BTPO

4.4.2 Characterisation of the prepared fibres

SEM

In the figure (4.18) we can see thinner and thicker fibres, the fibres don't contain defects, however they are not homogenous and thus the average size wasn't measured. There were no further fibre analysis of BTPO made due to a lack of the time and due to problems using measuring devices.

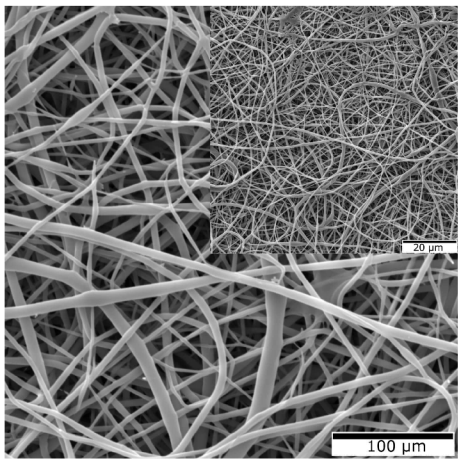

Figure 4.18: SEM of BTPO fibres.

4.5 *N,N′*-bis(3-(diethoxy(methyl)silyl)propyl)benzene-1,4-dicarboxyamide

4.5.1 Characterisation of the precursor

NMR

In the figure (4.19) below, we can see liquid state ^{1}H and ^{13}C NMR. The required structure is not pure in comparison to the other precursors and also it contains a much bigger amount of water (peak at 3.3 ppm). In the figure, we can see one more peak in ^{1}H and also in ^{13}C NMR, this is due to the presence of methyl functional group instead of ethoxy functional group.

Mass spectrometry

In the figure (4.20), the main masses observed are at 513.280 and 535.263. For the BiTSAP-b precursor, the theoretical mass (m/z) is 512.27. Therefore, the observed masses align well with the expected structure mass, whereby the predominant m/z found in the figure is the product with H^{+} or Na^{+}.

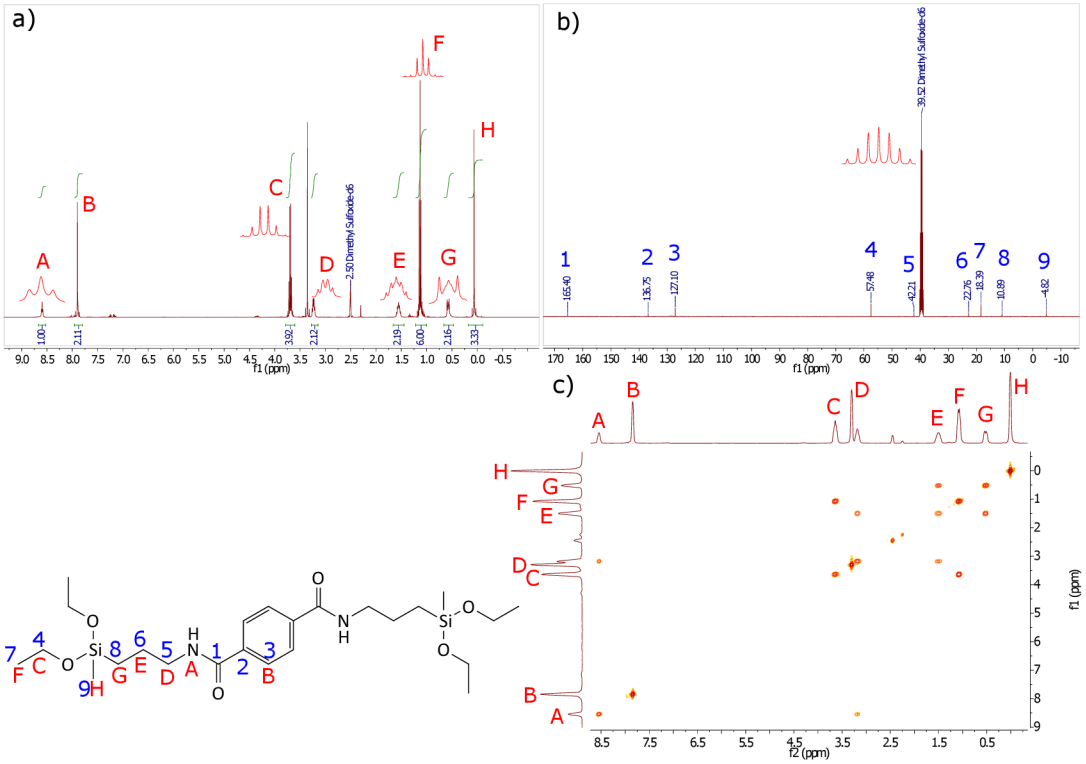

Figure 4.19: ^{1}H, ^{13}C and 2D COSY NMR of BiTSAB-b

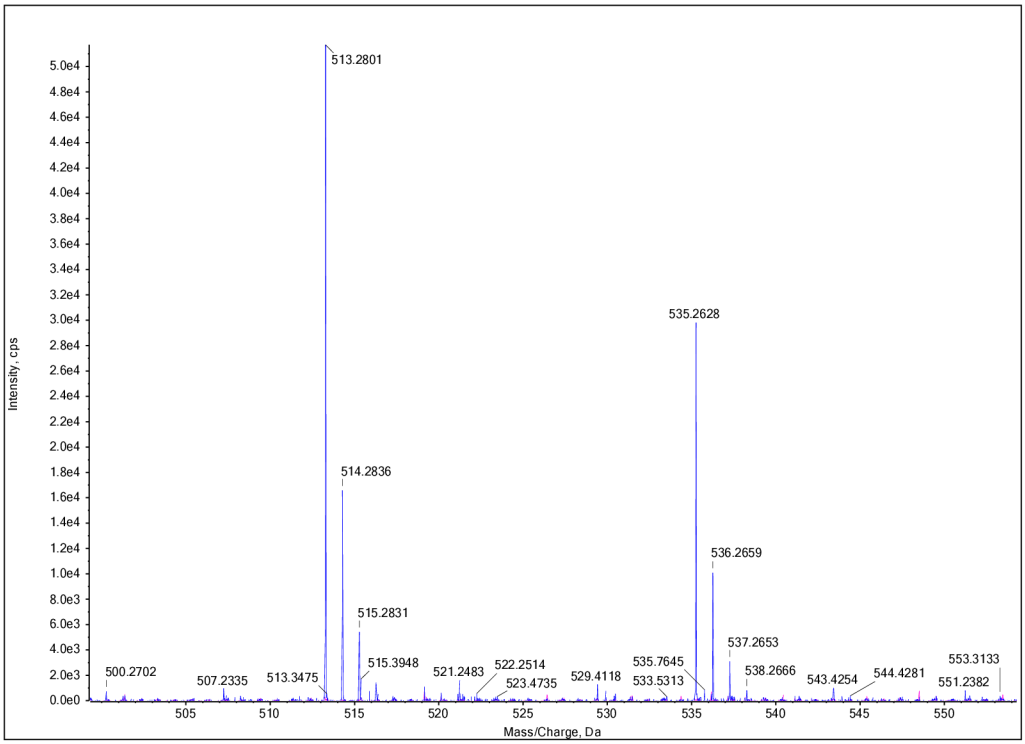

Figure 4.20: Mass spectrometry of BiTSAB-b

FTIR

In the figure (4.21) we can see water, Si−OH and −NH bonds around 3300 cm^{-1} present. Around 3000 cm^{-1} we can see aliphatic carbon chains $-CH_2-$ and $-CH_3$. Around 1700 to 1500 we can see peaks providing information about carbonyl and amide bonds. Around 1000 cm^{-1} are various types of silica bonds shown.

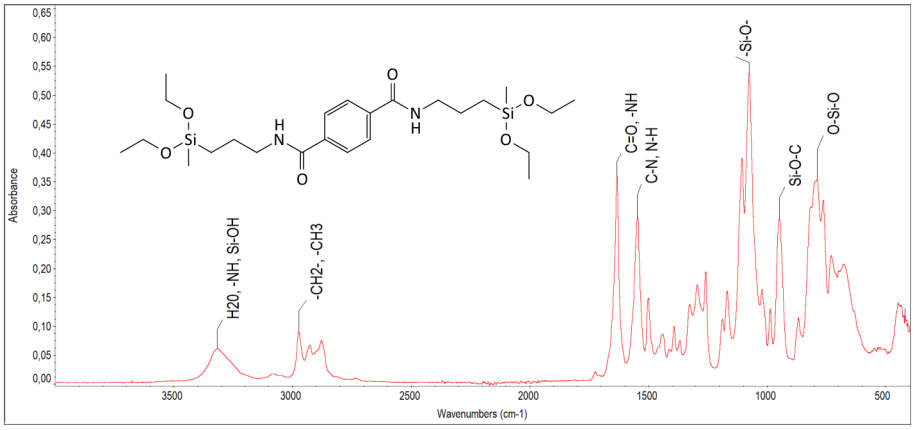

Figure 4.21: FTIR of BiTSAB-b

TGA

In the figure (4.22) we can see the main temperature intervals for decomposing - from 160.14 °C to 323.50 °C and from approximately 380 °C to 480.76 °C.

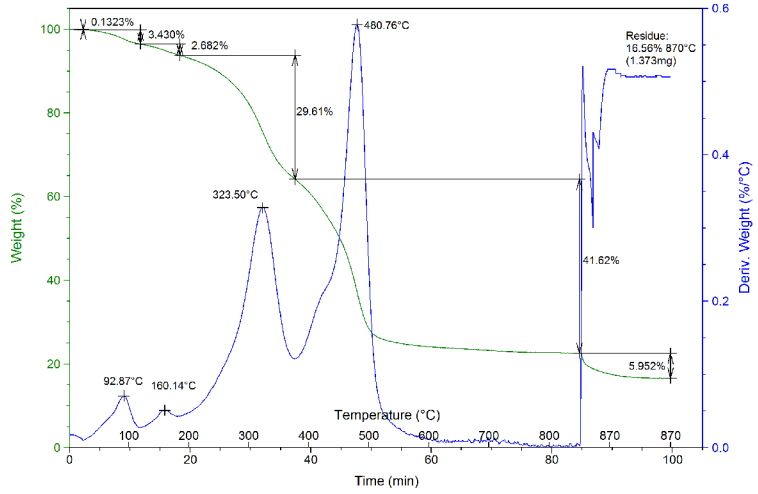

Figure 4.22: TGA of BiTSAB-b

4.5.2 Characterisation of the prepared fibres

SEM

In the figure (4.23) we can see thinner distributed fibres in comparison to the BiTSAB-a or BiTSAB-c. This can be due to use of a different electrospinning technique. The fibres look in general homogenous, smooth and without any visible defects. The size of the fibres was measured on 100 fibres and on average is 1 µm.

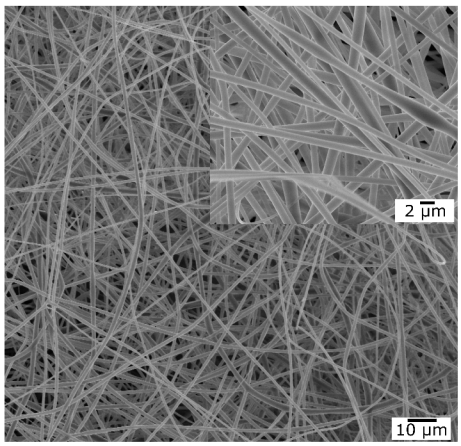

Figure 4.23: SEM of BTPO fibres

TGA of fibres

In the figure (4.24) we can see two temperatures - 39.75 °C and 339.68 °C. The product was not pure enough, because it already started decomposing at 39.75 °C.

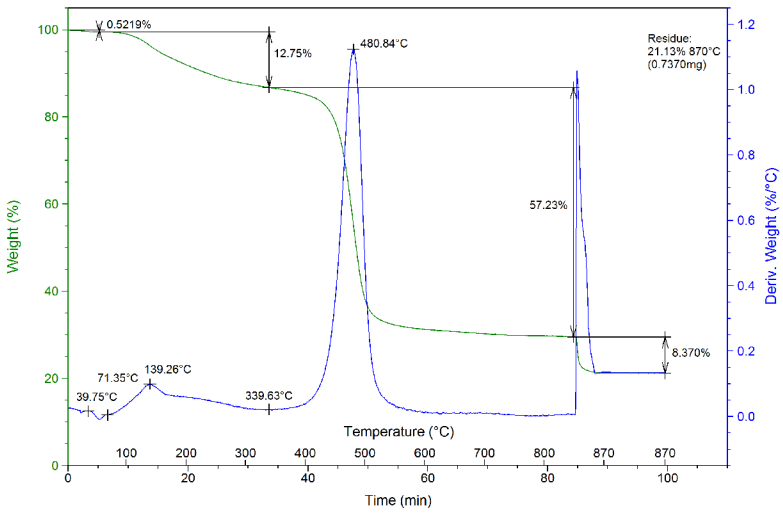

Figure 4.24: TGA of BiTSAB-b fibres

NMR of fibres

Fibres were subjected to solid state NMR which provides valuable information for the formed fibres such as the degree of polycondensation. From calculations using NMR spectral data, the degree of polycondensation was determined to be 67.2 %, with 32.1 % remaining ethoxy groups and thus 0.7 % of hydroxy groups. R in the figure of the molecule depicts the potential structure consisting of O−Si or O−CH_2CH_3 or −OH.

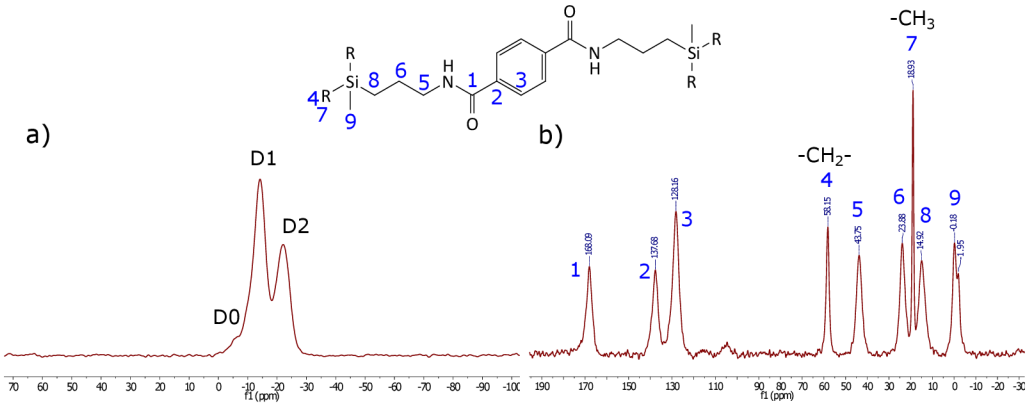

Figure 4.25: NMR of BiTSAB-b fibres

FTIR of fibres

For the comparison is in the figure (4.26) shown the FTIR spectrum of the precursor and of fibres made from the precursor. We can see that main structure stayed the same, but the peak around 1000 cm^{-1} got broader, this is due to growing Si-O-Si inorganic chain using sol-gel reaction.

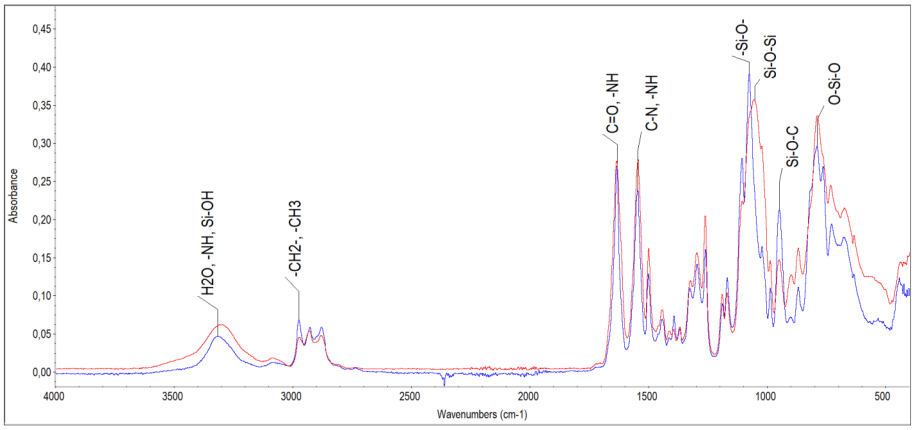

Figure 4.26: FTIR of BiTSAB-b fibres

4.6 *N,N′*-bis(3-(ethoxydimethylsilyl)propyl)benzene-1,4-dicarboxyamide

4.6.1 Characterisation of the precursor

NMR

In the figure (4.27) we can see liquid state ^{1}H and ^{13}C NMR. We can see that required structure is not pure, there can be seen many small peaks in the ^{13}C spectrum. We can see in ^{1}H spectrum big water content (peak at 3.3 ppm). In the figure, we can see one more peak in ^{1}H and also in ^{13}C NMR, this is due to the presence of two methyl functional groups instead of two ethoxy functional groups.

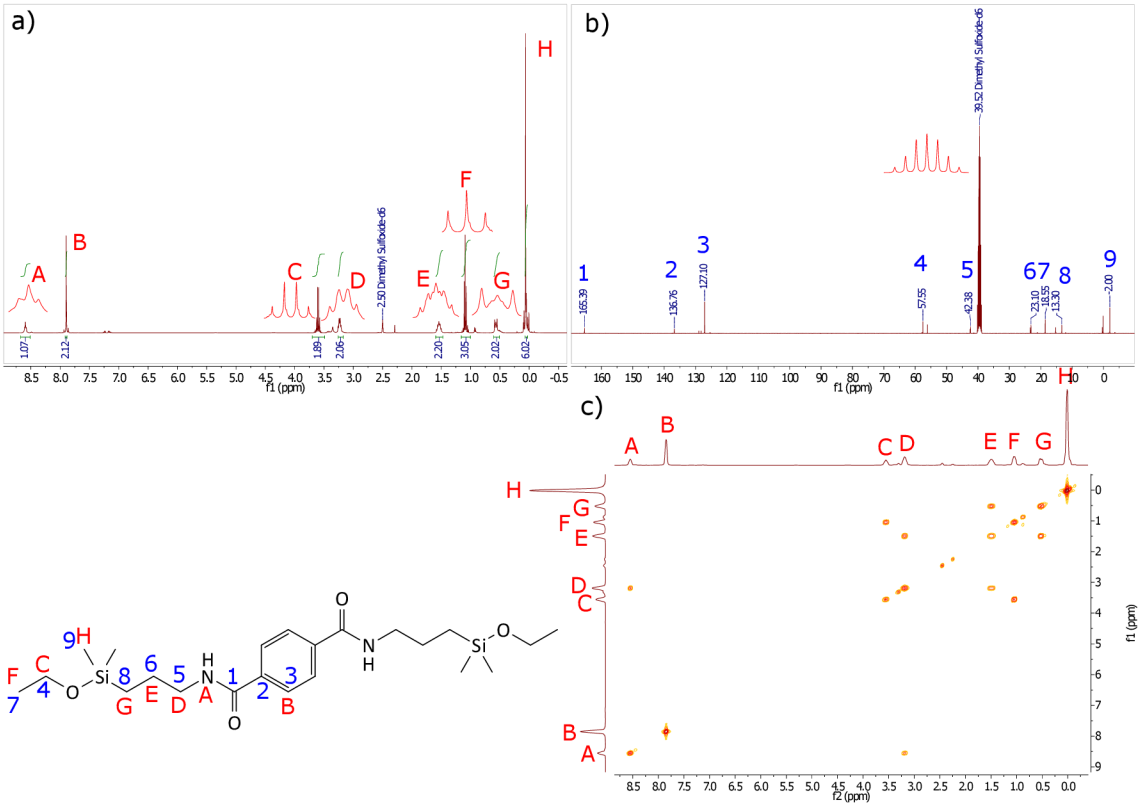

Figure 4.27: ^{1}H NMR, ^{13}C and 2D COSY NMR of BiTSAB-c

Mass spectrometry

In the figure (4.28), is the main mass observed at 453.258. For the BiTSAB-c precursor, the theoretical mass (m/z) is 452.25. Therefore, the observed masses align well with the expected structure mass, whereby the predominant m/z found in the figure is the product with H^{+} or Na^{+}. However in the figure can be seen many other fragments, which can indicate the unpurity of the synthesised precursor.

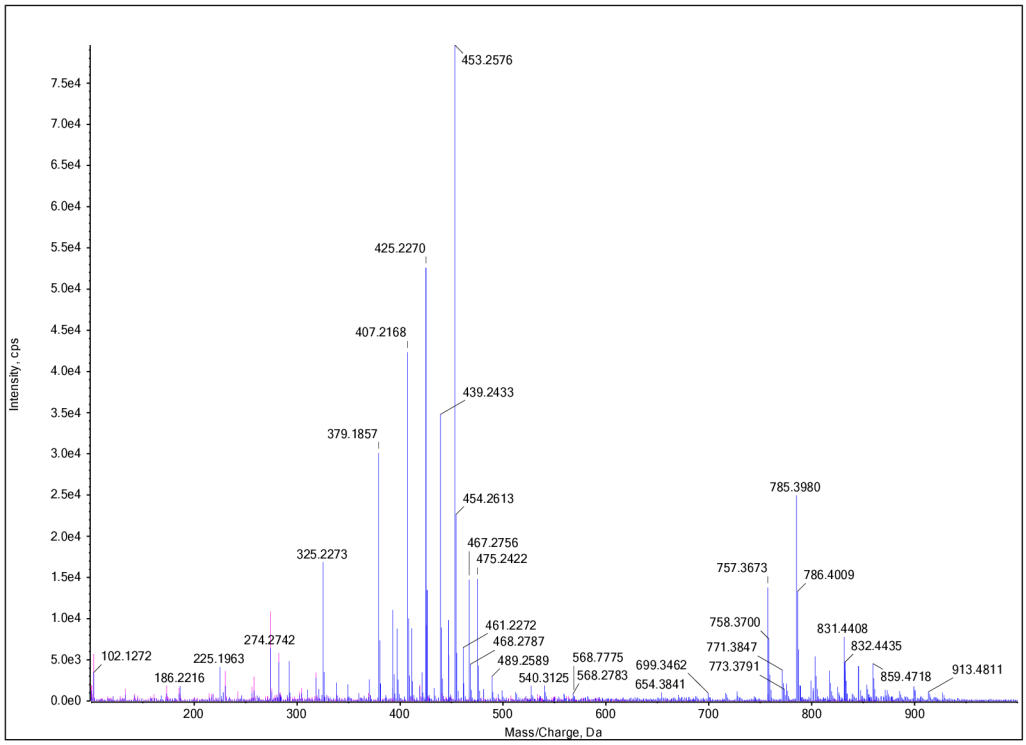

Figure 4.28: MS of *N,N′*-bis(3 (ethoxydimethylsilyl)propyl)benzene-1,4-dicarboxyamide

FTIR

In the figure below (4.29) we can see water, Si−OH and −NH bonds around 3300 cm^{-1} present. Around 3000 cm^{-1} we can see aliphatic carbon chains $-CH_2-$ and $-CH_3$. Around 1700 to 1500 we can see peaks providing information about carbonyl and amide bonds. Around 1000 cm^{-1} are various types of silica bonds shown.

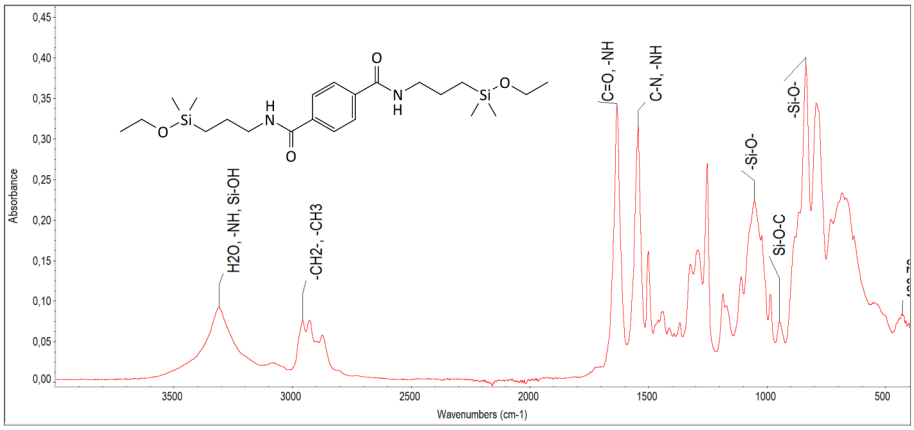

Figure 4.29: FTIR of BiTSAB-c

TGA

In the figure (4.30) we can see, that measured sample started decomposing at 124.47 °C and at 279.12 °C.

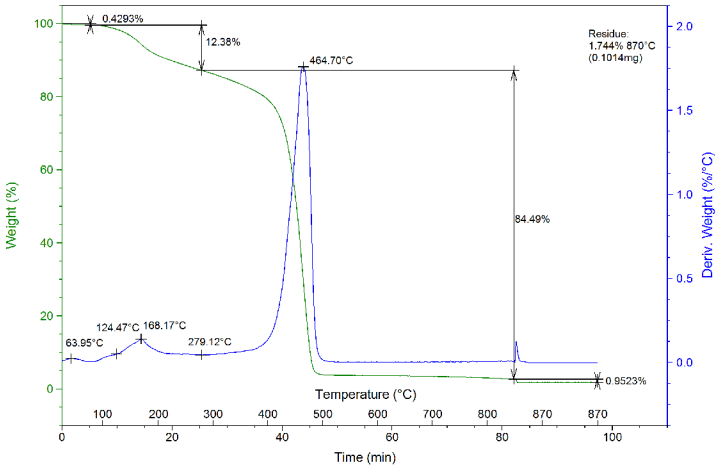

Figure 4.30: TGA of BiTSAB-c

4.6.2 Characterisation of the prepared fibres

SEM

In the figure (4.31) we can see fibres of the precursor BiTSAB-c. The fibres contain a lot of defects, are flat and wider in comparison to the previous precursor fibres. The fibres in the figure are not homogenous and thus the average size couldn't be measured. Due to the lack of time we couldn't measure solid state NMR, FTIR and TGA of the fibres. However, the fibres contain many defects, so these procedures are unsuitable at this moment.

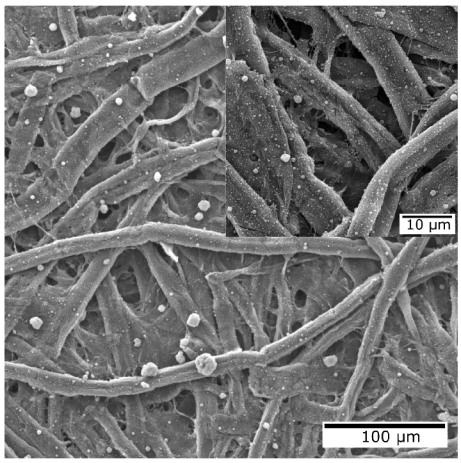

Figure 4.31: SEM of BiTSAB-c

5 Conclusion

In conclusion, this thesis shows the successful synthesis and characterisation of organo-bis-silylated precursors with different functional groups and organic components, known as organic bridges. The results demonstrate the successful synthesis of various organosilane molecules with the desired chemical structures, which were further utilized in electrospinning for the formation of (nano)fibres.

The research primarily focused on synthesis and characterisation of various organosilane components connected to a benzene organic component and subsequently their formation into (nano)fibres. However, due to constraints such as time limitations, the investigation was not fully completed. Nonetheless, the obtained findings can be used for future exploration and development in this area.

Future work and prospects for organosilanes should involve the exploration of novel structures incorporating diverse bridging organic linkers, which can result in superior properties of the final material. Specifically, a structure could be used which has a desired function and thus will allow the functionality to be exploited in the resulting fibres. Additionally, further studies should focus on characterisation of their properties and performance, investigating their potential applications based on formed structures.

Furthermore, understanding and controlling the sol-gel reaction mechanism represents a promising area for future exploration in the field of organosilanes. A deeper understanding and controlling of this mechanism will contribute to enhance the whole process and optimizing the properties of the resulting materials.

References

CARLOS, Luís, Rute FERREIRA, and Verónica BERMUDEZ, 2007. Hybrid Materials for Optical Applications. In: pp. 337–400. ISBN 978-3-527-31299-3. Available from DOI: 10.1002/9783527610495.ch9.

CROISSANT, Jonas G. et al., 2016. Organosilica hybrid nanomaterials with a high organic content: syntheses and applications of silsesquioxanes. *Nanoscale* [online]. Vol. 8, no. 48, pp. 19945–19972 [visited on 2022-12-07]. ISSN 2040-3364. Available from DOI: 10.1039/c6nr06862f.

ESCRIBANO, Purificación et al., 2007. Photonic and nanobiophotonic properties of luminescent lanthanide-doped hybrid organic–inorganic materials. *J. Mater. Chem.* Vol. 18. Available from DOI: 10.1039/B710800A.

FATIEIEV, Y. et al., 2015. Enzymatically degradable hybrid organic–inorganic bridged silsesquioxane nanoparticles for in vitro imaging. Nanoscale, 7(37), 15046-15050. [online] [visited on 2022-04-25]. Available from DOI: 10.1039/c5nr03065j.

GUASTAFERRO, Mariangela, E. REVERCHON, and L. BALDINO, 2021. Polysaccharide-Based Aerogel Production for Biomedical Applications: A Comparative Review. *Materials.* Vol. 14, p. 1631. Available from DOI: 10.3390/ma14071631.

HOFFMANN, Frank et al., 2006. Silica-Based Mesoporous Organic–Inorganic Hybrid Materials. *Angewandte Chemie International Edition* [online]. Vol. 45, no. 20, pp. 3216–3251 [visited on 2023-04-24]. ISSN 1521-3773. Available from DOI: 10.1002/anie.200503075.

HOLUBOVA, Barbora et al., 2020. Novel chapter in hybrid materials: One-pot synthesis of purely organosilane fibers. *Polymer* [online]. Vol. 190, p. 122234 [visited on 2022-12-08]. ISSN 0032-3861. Available from DOI: 10.1016/j.polymer.2020.122234.

HÜSING, Nicola, 2007. Porous Hybrid Materials. In: *Hybrid Materials: Synthesis, Characterization, and Applications*, pp. 175–223. ISBN 978-3-527-61049-5. Available from DOI: 10.1002/9783527610495.ch5.

JIANGYING, Xia et al., 2018. The transition from incoherent to coherent random laser in defect waveguide based on organic/inorganic hybrid laser dye. *Nanophotonics.* Vol. 7, pp. 1341–1350. Available from DOI: 10.1515/nanoph-2018-0034.

JUDEINSTEIN, Patrick and Clément SANCHEZ, 1996. Hybrid organic–inorganic materials: a land of multidisciplinarity. *Journal of Materials Chemistry* [online]. Vol. 6, no. 4, pp. 511–525 [visited on 2023-03-21]. ISSN 1364-5501. Available from DOI: 10.1039/JM9960600511.

KICKELBICK, Guido, 2007. Introduction to Hybrid Materials. In: *Hybrid Materials. Synthesis, Characterization, and Applications*, pp. 1–48. ISBN 978-3-527-61049-5. Available from DOI: 10.1002/9783527610495.ch1.

LOY, Douglas, 2007. Sol–Gel Processing of Hybrid Organic–Inorganic Materials Based on Polysilsesquioxanes. In: *Hybrid Materials: Synthesis, Characterization, and Applications*, pp. 225–254. ISBN 978-3-527-61049-5. Available from DOI: 10.1002/9783527610495.ch6.

LOY, Douglas A., 2018. Mesoporous Polysilsesquioxanes: Preparation, Properties, and Applications. In: KLEIN, Lisa, APARICIO, Mario, and JITIANU, Andrei (eds.). *Handbook of Sol-Gel Science and Technology: Processing, Characterization and Applications* [online]. Springer International Publishing, pp. 3177–3211 [visited on 2023-04-12]. ISBN 978-3-319-32101-1. Available from DOI: 10.1007/978-3-319-32101-1_131.

MAKOVA, Veronika, Barbora HOLUBOVA, Ilona KRABICOVA, et al., 2021. Hybrid organosilane fibrous materials and their contribution to modern science. *Polymer* [online]. Vol. 228 [visited on 2022-12-09]. ISSN 0032-3861. Available from DOI: 10.1016/j.polymer.2021.123862.

MAKOVA, Veronika, HOLUBOVA, Barbora, and KULHANKOVA, Johana, 2022. *Method for the Preparation of a Sol for the Preparation of Hybrid Organosilane Fibers by Electrostatic Spinning, the Sol Prepared by This Method and Hybrid Organosilane Fibers Prepared by the Electrostatic Spinning of This Sol*. Inventor: Veronika MAKOVA, Barbora HOLUBOVA, and Johana KULHANKOVA. Publ.: 2022-10. EP4067542 (A1). [Visited on 2023-04-25]. Available from: https://worldwide.espacenet.com/publicationDetails/biblio?FT=D&date=20221005&DB=&locale=en_EP&CC=EP&NR=4067542A1&KC=A1&ND=4.

MATERNE, Thierry, François de BUYL, and Gerald L. WITUCKI, 2012. Organosilane Technology in Coating Applications: Review and Perspectives [online] [visited on 2023-04-25]. Available from: https://www.academia.edu/10140050/Organosilane_Technology_in_Coating_Applications_Review_and_Perspectives.

OGOSHI, Tomoki and Yoshiki CHUJO, 2005. Organic–inorganic polymer hybrids prepared by the sol-gel method. *Composite Interfaces* [online]. Vol. 11, no. 8-9, pp. 539–566 [visited on 2022-12-15]. ISSN 0927-6440. Available from DOI: 10.1163/1568554053148735.

RAJABI, Fatemeh et al., 2020. Synthesis and Characterization of Novel Pyridine Periodic Mesoporous Organosilicas and Its Catalytic Activity in the Knoevenagel Condensation Reaction. *Materials*. Vol. 13, p. 1097. Available from DOI: 10.3390/ma13051097.

REN, Zhihui et al., 2021. Flexible Sensors Based on Organic–Inorganic Hybrid Materials. *Advanced Materials Technologies*. Vol. 6. Available from DOI: 10.1002/admt.202000889.

SANCHEZ, Clément, Kenneth J. SHEA, and Susumu KITAGAWA, 2011. Recent progress in hybrid materials science. *Chemical Society Reviews* [online]. Vol. 40, no. 2, pp. 471–472 [visited on 2022-12-15]. ISSN 1460-4744. Available from DOI: 10.1039/C1CS90001C.

WEI, Zhonglin et al., 2017. Thermally stable hydrophobicity in electrospun silica/polydimethylsiloxane hybrid fibers. *Applied Surface Science* [online]. Vol. 392, pp. 260–267 [visited on 2023-05-12]. ISSN 0169-4332. Available from DOI: 10.1016/j.apsusc.2016.09.057.